Mathematical modeling and optimal control analysis for the transmission risk of COVID-19

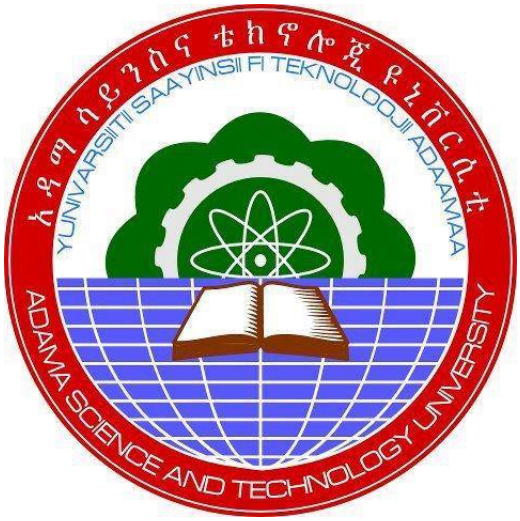

Dr. Legesse Lemecha and

Dr. Shiferaw Feyissa

Final research report submitted to School of Applied Natural Science
Adama Science and Technology University

September, 2022
Adama, Ethiopia

Mathematical modeling and optimal control analysis for the transmission risk of COVID-19

Dr. Legesse Lemecha and

Dr. Shiferaw Feyissa

Final research report submitted to School of Applied Natural Science
Adama Science and Technology University

September, 2022
Adama, Ethiopia

Acknowledgments

The authors would like to thank Adama Science and Technology University for financial support during this research work.

Abstract

*Coronavirus disease (COVID-19) is an infectious disease caused by SARS-CoV-2, a betacoronavirus. It is a pandemic disease affecting many countries. The present study was aims to investigate in the first phase the transmission risk of COVID-19 with optimal control. In the second case, to formulate and analyze a mathematical model of COVID-19 transmission dynamics and apply it as case study in Ethiopia. Accordingly, we apply optimal control theory to a novel coronavirus(COVID-19) transmission model given by a system of nonlinear ordinary differential equations. An expression for the basic reproduction number is derived in terms of control variables. Then the sensitivity of basic reproduction number with respect to model parameters is also analyzed. Optimal control strategies are obtained by minimizing the number of exposed and infected population considering the cost of implementation. The existence of optimal controls and characterization is established using Pontryagin's Minimum Principle. Numerical simulation results demonstrated good agreement with our analytical results. Finally, the findings of this study shows that comprehensive impacts of prevention, intensive medical care and surface disinfection strategies outperform in reducing the disease epidemic with optimum implementation cost. In the second phase, we proposed a nonlinear deterministic mathematical model for the transmission dynamics of COVID-19. Then, we analyzed the system properties such as boundedness of the solutions, existence of disease-free and endemic equilibria, local and global stability of equilibrium points. Besides, we computed the basic reproduction number R_0 and studied its normalized sensitivity for model parameters to identify the most influencing parameter. The local stability of the disease-free equilibrium point is also verified via the help of the Jacobian matrix and Routh Hurwitz criteria. Moreover, the global stability of the disease-free equilibrium point is proved by using the approach of Castillo-Chavez and Song. We also proved the existence of the forward bifurcation using the center manifold theory. Then the model is fitted with COVID-19 infected cases reported from March 13, 2020, to July 31, 2021, in Ethiopia. The values of model parameters are then estimated from the data reported using the least square method together with the fminsearch function in the **MATLAB** optimization toolbox. Finally, different simulation cases were performed using PYTHON software to compare with analytical results. The simulation results suggest that the spread of COVID-19 can be managed via minimizing the contact rate of infected and increasing the quarantine of exposed individuals.*

Keywords: COVID-19; Mathematical modelling; basic reproduction number; stability; bifurcation;sensitivity analysis; optimal control.

Original results

This research report presents two original results that contribute to the expansion of the frontiers of knowledge and scientific development of Mathematics. The original contributions of this research work were already published in international peer-reviewed journals indexed both in Web of Science and Scopus. The contributions are:

P1) Legesse Lemecha and Shiferaw Fiyissa: Optimal control strategies for the transmission risk of COVID-19, Journal of Biological Dynamics, Vol.14(1), 590-607, 2020 https://doi.org/10.1080/17513758.2020.1788182

P2) Zenebe Shiferaw Kifle, Legesse Lemecha Obsu: Mathematical modeling for COVID-19 transmission dynamics: A case study in Ethiopia. Results in Physics 34(2022)105191; doi.org/10.1016/j.rinp.2022.105191;

Contents

List of Tables

List of Figures

ACRONYMS

COVID-19	Coronavirus disease 2019
SARS-CoV-2	Severe Acute Respiratory Syndrome Coronavirus 2
WHO	World Health Organization
CDC	Center for Disease Control
NPI	Non-Pharmaceutical Interventions
EPHI	Ethiopian Public Health Institute

CHAPTER 1

INTRODUCTION

1.1 Background of the study

Coronaviruses are a family of viruses that circulate among animals and sometimes can also be found in humans.The new virus was first appeared late December 2019 in the Chinese city of Wuhan and eventually invaded the world due to fast modern air transportation. The novel coronavirus- now referred to as COVID-19 is caused by severe acute respiratory syndrome(SARS-CoV-2) and consists of single-stranded ribonucleic acid (RNA) structure (Catrin Sohrabi & Agha., 2020). According to the World Health Organization(WHO) situation report, worldwide, more than 5, 934, 936 people were infected and about 367, 166 were expired due to COVID-19 virus infection between December 2019 and May 31, 2020 (Organization, 2020). The rapid geographically spread of the disease and induced deaths are continued to rise mortality rate of about 5% (R. Li et al., n.d.).The extremely spread of the disease and lack of approved medicine make the disease a challenging problem for public health organizations (Hanscheid et al., 2020).

The novel coronavirus can cause mild, non-specific symptoms, including fever, cough, shortage of breath, muscle pain and tiredness similar to those caused by SARS-CoV and MERS-CoV infections(Gralinski & Menachery, 2020). In more serious cases, it can develop severe pneumonia, acute respiratory distress syndrome, sepsis and septic shock that can lead to death. The virus is transmitted via respiratory droplets produced when an infected person coughing, sneezing, and during talking in a social distance less than a meter. The estimated incubation period is 2-14 days, but could be longer (Yang & Wang, 2020). The virus is most contagious when infected people are symptomatic, although spread may be possible before symptoms appear(Rothe et al., 2020).

The review given in (Kampf et al., 2020) reveals that human coronaviruses such as(SARS), (MERS) or endemic human coronaviruses (HCoV) can persist on inanimate surfaces like metal, glass or plastic for up to 9 days at room temperature and the duration of persistence is shorter when a temperature is greater than or equal to 30°C. The study also provided strong evidences for the pathogen's environmental survival which can be inactivated by surface disinfection procedures with 62-71% ethanol, 0.5% hydrogen peroxide or 0.1% sodium hypochlorite within 1 minute. In order to deal with the epidemic of COVID-19, governments have implemented various control measures such as home quarantine, spray disinfectant, isolation and suspend all public traffics within their cities (Lin et al., 2020; Pan et al., 2020).

Mathematical modelling plays an important role in comprehending and providing useful techniques to predict and control the dynamics of infectious disease(Hethcote, 2000). In the

past few decades, several researchers have developed various mathematical models to investigate the transmission dynamics of infectious diseases and its control measures, for example, see in (E. Ahmed & El-Saka, 2017; Y. Kim et al., 2016; Lee et al., 2017; Tahir et al., 2019; Van den Driessche & Watmough, 2002) and references cited therein. Tang, Wang, et al. (2020) considered a general SEIR-type epidemiological model to estimate the transmission risk of COVID-19 and its implication by taking into consideration: clinical progression of disease, individual epidemiological status, and the intervention measures. The control reproductive number is found to be 6.47. Sensitivity analyses also show that interventions can effectively reduce the control reproduction number and transmission risk. Later, this study was generalized by using time-dependent contact and diagnose rates in(Tang, Bragazzi, et al., 2020). Wu et al. (2020), proposed SEIR epidemic model to simulate the transmission dynamics, and forecast the potential domestic and global spread of the COVID-19 outbreak originated in Wuhan, China. They estimated that the basic reproductive number for COVID-19 was about 2.68. In addition,(Lin et al., 2020) proposed a conceptual SEIR model for the coronavirus disease (COVID-19) outbreak in Wuhan, China considering individual reaction and governmental action. The proposed model also demonstrated effectively the trends of COVID-19 outbreak. Kucharski et al. (2020) studied early transmission dynamics and control of COVID-19 by considering a stochastic transmission model with real data from Wuhan outbreak. A similar study also presented in (Chen et al., 2020; Mizumoto & Chowell, 2020). In all these studies conducted on COVID-19, detailed mathematical analysis is not presented.

At global level, the outbreak of unexpected infectious diseases causes several impacts on the economic sector. For instance, the first visible impact could be preventive and containment measures taken by governments using their limited resources. For effective utilization of limited resources, using the techniques of optimal control can play paramount role during intervention period. Optimal control theory has been widely applied to Ebola, Zika, HIV,and TB mathematical models (see, e.g., (Area et al., 2017; Khan et al., 2019)and references cited therein). Some of these authors were applied optimal control techniques in order to understand how the spread of these diseases may be controlled, e.g., through education campaigns, vaccination, treatment, quarantine or isolation with optimal implementation costs. In Lee et al. (2017), the authors introduce a deterministic mathematical model for the MERS-CoV outbreak in South Korea with additional hospitalization and contact components in order to understand the disease dynamics. Optimal control strategies, both in the case of hospitalization and contact are used to predict the possible future outbreak in terms of resource utilization for disease control. While there are relatively vast literature on the application of optimal control in epidemiology, results in novel coronavirus are almost nil.

In thier study, Yang & Wang (2020) proposed a mathematical model to investigate the ongoing novel coronavirus epidemic in the Chinese city of Wuhan. The model has two unique features: the incorporation of an environmental reservoir into the disease transmission dynamics, and the use of non-constant transmission rates which change with epidemiological status and environmental conditions. Global stability was analyzed using Lyapunov function. The model was fitted with real data from Wuhan epidemic report. However, nothing has been said about sensitivity of model parameters and optimal intervention of the disease. The first part of the present study addresses this gap. Furthermore, in the study (Bajiya et al., 2020), the mathematical modeling of COVID-19 is proposed and analyzed. But in their study, they did not considered the class of asymptomatically infected individuals. Besides, Deressa & Duressa (2021) studied a mathematical modeling of COVID-19 by extending the SEIR model with asymptomatic and hospitalized class. But in their study, they did not considered the class of quarantined and disease induced death rate in the asymptomatic. Thus, in the second phase of this study, we formulated and analyzed a mathematical model of COVID-19 by extending the SEIR model to quarantined, hospitalized and asymptotically infected individuals.

1.2 Statement of the problem

COVID-19 is the infectious disease caused by the most recently discovered coronavirus. This new virus and disease were unknown before the outbreak began in Wuhan, China, in December 2019. COVID-19 is now a pandemic affecting many countries globally and affects all age groups. According to the World Health Organization(WHO) situation report-132, globally, more than 5, 934, 936 people were infected and about 367, 166 life were lost due to COVID-19 disease between December 2019 and May 31, 2020. From these, 100, 610 confirmed cases and 2, 554 deaths were reported from Africa (Organization, 2020). Also, Ethiopia contributes, 1,063 confirmed cases and 8 deaths at national level. On June 1, 2020, the confirmed cases were increased to 1,257 while total deaths equals 12.

The United Nations Economic Commission for Africa has estimated that anywhere between 300,000 and 3.3 million African people could lose their lives as a direct result of COVID-19, depending on the intervention measures taken to stop the spread (Massinga Loembé et al., 2020). According to this report, Africans are susceptible because 56 per cent of the urban population is concentrated in overcrowded and poorly serviced slum dwellings (excluding North Africa) and only 34 per cent of the households have access to basic hand washing facilities. In the report, the economic impact due to COVID-19 estimated that African economies could be the slowing of growth to 1.8 per cent in the best case scenario or a contraction of 2.6 per cent in the worst case. This has the potential to push 27 million people into extreme poverty.

As cited and explained in (Ethiopia, 2020), UNECA has estimated that due to the COVID-19

crisis 48 percent fewer people could be lifted out of poverty in the continent and the projection of this estimate on Ethiopia situation with the same rate shows that (based on the progress made by the country during the period 2010/11-2015/16) additional 600,000 people per year will fall in absolute poverty measured according to national definition. From these recent reports, it is evident that the consequence of COVID-19 is very dangerous both in terms of health crisis and socio-economic impact unless appropriate mitigation strategies are studied and designed in Ethiopian context.

Mathematical models for COVID-19 infection can provide better insights into the dynamics of virus and play a significant role in designing better control strategies. Thus, in the first part of this project we investigated an optimal control strategies for the transmission risk of COVID-19 by taking into account the effect of awareness in COVID-19 crises management, social distancing, and environmental disinfectants. In the second phase, we developed new mathematical model and apply it to predict the tends of epidemic. For this, we studied existence and stability criteria of the equilibria in terms of the basic reproduction number. Then we performed sensitivity of reproduction number with respect to model parameters. Finally, we fitted the formulated model parameters with real data from Ethiopia.

1.3 Objectives of the study

1.3.1 General objective

The general objective of this study is to propose a mathematical model with optimal control that could describe the transmission risk of coronavirus (COVID-19).

1.3.2 Specific objectives

The specific objectives of the study are to:

(a) formulate a mathematical model with optimal control describing the transmission risk of COVID-19.

(b) propose and analyze optimal control strategies that are used to minimize the spread of coronavirus with optimal implementation cost.

(c) formulate and analyze a mathematical model that describe the transmission dynamics of COVID-19,

(d) fit the formulated model parameters with real data on COVID-19 extracted from Ethiopia,

1.4 Significant of the study

A well studied and organized research report on COVID-19 provides strong information on how to design appropriate control and preventive measures in order to bring a long term solution. Thus, the outcome of this study are helpful to:

(a) create awareness on the impact of COVID-19 and its prevention,

(b) pave away to suggest appropriate intervention mechanisms,

(c) predict the epidemic of coronavirus infectious and to take precautionary measures

(d) guide policy makers in making appropriate intervention with optimal implementation cost.

(e) the findings of this study also helps to improve decision making at strategic level and adds advantage of interpret the situation of the coronavirus disease

(f) motivate other researchers for further study and mathematical analysis.

1.5 Ethical issues

The present study involves people that are: susceptible, exposed, infectious, hospitalized, recovered from the diseases. It contains only general research work that does not involve any kind of risk for its development. Moreover, the researcher is committed to follow all ethical issues during this studies as per the rules and regulation of Adama Science and Technology University.

CHAPTER 2

LITERATURE REVIEW

Mathematical modeling of infectious disease is used as a powerful tool for studying the dynamics of disease transmission and the effect of different intervention strategies to inform public health policy makers on the implementation of effective intervention programs to combat infections. In 1927, Kermack and McKendrick introduced a prominent compartmental model to analyze the plague disease in Mumbai and succeeded in revealing its epidemiology (Kermack & McKendrick, 1927). After that, mathematical modeling have been playing a significant role in analyzing the spread and control of different infectious diseases (Anderson et al., 1992; Castillo-Chavez & Song, 2004).

2.1 Reviewed literature on COVID-19 models

Coronavirus disease is a communicable disease caused by a family of novel coronavirus. The virus is referred to as severe acute respiratory syndrome coronavirus 2 (SARS-CoV-2) and the associated disease is COVID-19 (Ge et al., 2020). This newly discovered family of novel coronavirus disease started in Wuhan, Hubei Province, China, in late December 2019 and spread rapidly around the world, causing major public health concerns (Q. Li et al., 2020; Nadim & Chattopadhyay, 2020; Wu et al., 2020). In January 2020, the new virus was named the 2019 novel coronavirus, and later, it was renamed as Coronavirus Disease 2019 (COVID-19) by World Health Organization (WHO) in February 2020 (Catrin Sohrabi & Agha., 2020; Hui et al., 2020). The rate of infection of the disease was very high as a result, WHO has declared it as a pandemic on March 11, 2020 (Cucinotta & Vanelli, 2020). Most people infected with the COVID-19 virus experience mild to moderate respiratory illness and recover without requiring special treatment. However, people having medical problems (cardiovascular disease, diabetes, chronic respiratory disease, cancer) and older people are more likely to develop serious illnesses. Globally, the COVID-19 pandemic infected more than 197 million individuals up to the end of July 2021, and among these more than 4 million individuals have died.

The symptoms of COVID-19 are variable, ranging from mild symptoms to severe illness. The clinical symptoms of COVID-19 include fever, dry cough, fatigue, sore throat, diarrhea, loss of taste or smell, and headache. In severe cases, it may result in difficulty breathing or shortness of breath, chest pain or pressure, and loss of speech (Authority et al., 2021). The estimated incubation period is 2–14 days after contact, but it might extend up to 27 days (Worldometer, 2020). Moreover, asymptomatic individuals do not develop any symptoms and not aware of their infection, yet they are capable of transmitting the disease (Rothe et al., 2020). COVID-19 by its nature very contagious and spread easily from person to person. Most commonly it transmit from

person to person via respiratory droplets produced when an infected person coughing, or sneezing within a social distance less than 6 feet (CDC, 2019).

The first case report of COVID-19 in Ethiopia was on March 13, 2020, two days after the global pandemic was declared. Then on April 16, 2020, the Ethiopian Public Health Institute reported a total of 92 confirmed cases, three deaths and two recoveries(Debela, 2020). Thereby, the Federal Government of Ethiopia declared lock down, imposed quarantine for all travelers, restricted public gatherings, and school closures to combat the pandemic. Besides, the government announced intensively through mass media, social media and cell-phone ring to keep physical distance, wear face masks, and to keep their personal hygiene. Moreover, the Minister of Health was also started daily briefings on the disease progress. In-between, the national politics spoiled and people neglect following COVID-19 protocol. As a consequence, the disease spread throughout the country and continued claiming many lives. In addition to weak health care system, many Ethiopians live in poor and crowded conditions (Mussie et al., 2020) in large cities. This would further facilitate the spread of the disease. For instance, up to July 31, 2021, the total confirmed and death cases reported due to COVID-19 in Ethiopia, respectively, are 280,365, and 4,385 (Yazew et al., 2021). Furthermore, peoples' awareness on the COVID-19 is very weak and wearing face mask is also almost nil in the countryside.

Mathematical modeling plays a fundamental role in understanding, predicting, and controlling the transmission dynamics of infectious diseases. In this regard, its application has a long history, for example, in malaria (Cai et al., 2017; Makinde & Okosun, 2011; Mohammed-Awel & Gumel, 2019), tuberculosis (Das et al., 2020; S. Kim et al., 2018), and references cited therein. Since COVID-19 outbreak, many mathematicians studied the transmission dynamics of the disease considering different scenarios (Aldila et al., 2020; Ali et al., 2020; Bajiya et al., 2020; Bugalia et al., 2020; Yang & Wang, 2020). In particular, Yang & Wang (2020) proposed and analyzed a mathematical model for COVID-19 incorporating multiple transmission pathways, including both human-to-human and environment-to-human transmission routes. Ali et al. (2020) proposed a mechanistic model to investigate the role of asymptomatic class, quarantine, and isolation in the transmission dynamics of COVID-19. They have performed a detailed theoretical analysis in terms of the basic reproduction number and predicted cumulative cases. Moreover, the study suggests that quarantine and isolation of individuals play a significant role in controlling the transmission of the disease.

Bugalia et al. (2020) proposed a mathematical model to study the transmission dynamics of COVID-19 considering the role of social distancing, lockdown, quarantine, and isolation. The result of this study reveals that reducing the contacts through increasing the efficacy of

lockdown and quarantine of asymptomatic individuals significantly minimized the epidemic of the disease. In (Aldila et al., 2020), a mathematical model for COVID-19 is proposed by taking into consideration pharmaceutical and non-pharmaceutical intervention techniques to combat the pandemic of novel coronavarious. The authors estimated model parameter values using real data reported on COVID-19 from three provinces in Indonesia, namely, Jakarta, West Java, and East Java. Moreover, they implemented the theory of optimal control to determine the best intervention strategies with optimal cost. Their results showed that community awareness plays a crucial role in the success of COVID-19 eradication programs.

In the case of Ethiopia, a limited number of mathematical models on COVID-19 outbreak have been studied with real data. Haileyesus and Getachew considered a SEIR compartmental model and extended the model into optimal control to investigate the dynamics of the disease (Tilahun & Alemneh, 2021). In (Deressa & Duressa, 2021), Chernet and Gemechis proposed and analyzed an extension of the SEIR model to asymptomatic and hospitalized classes. Moreover, they presented a detail analysis and fitted the model to real data from Ethiopia. Their study concluded that the combined effects of public health education, personal protective, and treatment of hospitalized individuals are significantly reducing the expansion of the disease. However, the authors do not consider quarantined individuals and disease-induced death rate in asymptomatic compartment. Cases are not fully reported due to weak health infrastructure and limited well trained human power in the country. The asymptomatic individuals are identified as an important source of disease transmission and isolated infected individuals is a primary mechanism adopted to control the spread of the disease (CDC, 2019). Thus, this study aims to study the transmission dynamics of COVID-19 via extending the SEIR model by including asymptomatic, quarantined, and hospitalized classes. The model parameters are fitted to the reported real data of COVID-19 from March 13, 2020 to July 31, 2021 in Ethiopia.

Since COVID-19 outbreak, many mathematicians studied the transmission dynamics of the disease considering different scenarios (Ali et al., 2020; Bajiya et al., 2020; Bugalia et al., 2020; Eikenberry et al., 2020; Ullah & Khan, 2020; Yang & Wang, 2020). In particular, Yang & Wang (2020) proposed a mathematical model for COVID-19 incorporating multiple transmission pathways, including both human-to-human and environment-to-human transmission routes. The authors employed a bilinear incidence rate based on the law of mass action and fitted the model to the data of Wuhan city of China and estimated the reproduction number. They found that the contribution of the environmental reservoir is significant in shaping the overall disease risk. Their results also indicate that the COVID-19 infection remain endemic, which necessitates intervention programs and long-term disease prevention policies. Further, Bugalia et al. (2020) proposed a mathematical model to study the transmission dynamics of COVID-19 considering the role

of social distancing, lockdown, quarantine, and isolation. The result of this study reveals that reducing the contacts through increasing the efficacy of lockdown and quarantine of asymptomatic individuals significantly minimized the epidemic of the disease.

Moreover, Bajiya et al. (2020) studied the impact of non-pharmaceutical interventions on the dynamics of COVID-19 using a mathematical model. They employed a mixing standard incidence rate based on the law of mass action and estimated parameter values using case data reported on COVID-19 from India. Their study suggests that the efficiency of non-pharmaceutical interventions (NPI) is one of the vital factors to control the disease spread in the COVID-19 outbreak situation in India. Further, to enhance the idea of NPIs, their study demonstrates that employing more than one improved NPIs at the same time is better than one NPI for the COVID-19 control in India. Furthermore, Eikenberry et al. (2020) designed a mathematical model to study the potential impact of the use of face-masks by the public to curtail the spread of the COVID-19 pandemic. Their results suggest that the use of face masks by public is potentially of high significance in curtailing the burden of the pandemic. The community-wide benefits are likely to be greatest when face masks are used in conjunction with other non-pharmaceutical practices (such as social or physical distancing), and high universal adoption and compliance.

Recently, there were several epidemiological modeling studies that have been done to explore the transmission dynamics of COVID-19 pandemic (Memon et al., 2021; Musa et al., 2021; Ngonghala et al., 2020; Tang, Wang, et al., 2020). For instance, Tang, Wang, et al. (2020) developed and analyzed a deterministic model which incorporates quarantine and hospitalization to estimate the transmission risk of the COVID-19 and its implication for public health interventions. Their model was further extended by Ngonghala et al. (2020) by dividing infectious compartment into two essential compartments of hospitalized or isolated individuals and those in intensive care units to assess the impact of NPI on curtailing the spread of COVID-19 pandemic. Memon et al. (2021) formulated a new COVID-19 model of deterministic type to assess role of quarantine and isolation for effective control of the epidemic in Pakistan. They carried out theoretical analysis of the model with discussion of existence, uniqueness, boundedness and equilibria of the model. They estimated the value for R_0 about 1.31 which indicates persistence of the epidemic in the country. Based on real data for active cases in the country, they suggested some increase in the quarantine period as the effective tool to fight with the ongoing epidemic of COVID-19. Musa et al. (2021) proposed a mathematical modeling of COVID-19 epidemic with effect of awareness programs in Nigeria. Their model incorporates awareness programs and different hospitalization strategies for mild and severe cases, to assess the effect of public awareness on the dynamics of COVID-19 infection. They found that the epidemic could increase if awareness programs are not properly adopted. Further, their results suggest that the awareness programs and timely

hospitalization of active cases are essential tools for effective control and mitigation of COVID-19 pandemic in Nigeria and beyond.

2.2 COVID-19 models with optimal control

Following the outbreak of the COVID-19 disease many optimal control models have been formulated and analyzed. For instance, Legesse & Shiferaw (2020) extended the model proposed by Yang & Wang (2020) by applying an optimal control model to minimize the transmission risk of COVID-19. They showed that comprehensive impacts of prevention, intensive medical care and surface disinfection strategies outperform in reducing the disease epidemic with optimum implementation cost. In (Aldila et al., 2020), a mathematical model for COVID-19 is proposed by taking into consideration pharmaceutical and non-pharmaceutical intervention techniques to combat the pandemic of novel coronavirus. The authors estimated model parameter values using real data reported on COVID-19 from three provinces in Indonesia, namely, Jakarta, West Java, and East Java. Moreover, they implemented the theory of optimal control to determine the best intervention strategies with optimal cost. Their results showed that community awareness plays a crucial role in determining the success of COVID-19 eradication programs. Further, Ali et al. (2020) proposed a deterministic compartmental model to investigate the role of asymptomatic class, quarantine and isolation in the transmission dynamics of COVID-19. They have performed a detailed theoretical analysis in terms of the basic reproduction number and predicted the cumulative cases. Moreover, in their paper, they uses optimal control theory to find quarantine (for susceptible and exposed) and isolation strategies that would minimize the total infected population and while using optimum resources. Their study suggests that quarantine and isolation of individuals play a significant role in controlling the transmission of the disease.

Moreover, Ullah & Khan (2020) proposed a mathematical model to analyze the dynamics and impact of non-pharmaceutical interventions on the COVID-19 in Pakistan. First, they developed a model without optimal control variables and provided a good fit to the reported cases data. Later, they reformulated the proposed model by incorporating two control functions in order to determine an appropriate innervation mechanisms. They observed that the most effective strategy to minimize the disease burden is the implementation of maintaining a strict social-distancing and contact-tracing to quarantine the exposed people. Olaniyi et al. (2020) formulated a nonlinear deterministic epidemic model for COVID-19 incorporating transmission routes from three infectious classes, including symptomatic, asymptomatic, and hospitalized individuals. The model is parameterized and analyzed based on the cumulative number of reported active cases in Nigeria. Moreover, in their study optimal control theory is applied to the epidemiology of COVID-19 transmission in order to assess the optimal levels of time-dependent prevention and management measures that will significantly minimize the number of infectious humans in the population. They showed that the optimal preventive measure is better than management control

in reducing the burden of the disease, but the combined effort of the two controls has significant effect in reducing the number of infectious individuals in the population. Furthermore, Deressa & Duressa (2021) proposed and analyzed an extension of the SEIR model to asymptomatic and hospitalized classes. They presented a detailed analysis and fitted the model to real data from Ethiopia. Their study concluded that the combined effects of public health education, personal protection, and treatment of hospitalized individuals are significantly reducing the expansion of the disease.

Thus, in Chapter 4 we investigated an optimal control strategies for the transmission risk of COVID-19 by taking into account the effect of awareness in COVID-19 crises management, social distancing, and environmental disinfectants. In Chapter 5, we developed new mathematical model and apply it to predict the tends of epidemic. For this, we studied existence and stability criteria of the equilibria in terms of the basic reproduction number. Then we performed sensitivity of reproduction number with respect to model parameters. Finally, we fitted the formulated model parameters with real data from Ethiopia.

CHAPTER 3

RESEARCH METHODOLOGY

In this chapter, we present the methods and materials that are used to attain the general and specific objectives stated in Section 1.3. For this, we briefly discuss: source of data, method of data analysis, the approach of study and mathematical procedures.

3.1 Source of data and data collection

3.1.1 Source of data

In this study, to acquire the desired knowledge on the dynamics of the disease secondary source of information were collected both from published and unpublished documents. That is, the source of information that is used in this study are WHO situation reports, Worldometers and Johns hopkins university corona virus resource center.

3.1.2 Data collection

Data collection is the process of gathering and measuring information on targeted variables in an established systematic fashion, which then enables one to answer relevant questions and evaluate outcomes. It is useful to distinguish between two broad types of variables: qualitative and quantitative. For this research we collected numerical data. The data play an important role in increasing the validity, accuracy and reliability of the research. The time series data was collected on daily records of the patients from 13 march, 2020 to 31 July, 2021 in Ethiopia.

3.1.3 Data analysis

Data analysis is the process of analyzing collected data to outdraw meaningful insights. The techniques focus on the statistical, or mathematical analysis of the data sets, using computational techniques and algorithm. As our data points are taken over time, time series analysis method is used to analyze the data. We fed our data into the dynamical model to find critical patterns and trends, to explain certain phenomena or to make predictions on how the dynamical state variables of interest may fluctuate in the future. For parameter estimation, we used least square techniques. The parameters value obtained is then used as a baseline parameter value that is applied in the numerical simulations. The study involves both qualitative and quantitative analysis. The numerical simulation is conducted using MATLAB software and the results is displayed in the form of figures.

3.2 Mathematical procedures

In this study, first we extended the mathematical model introduced in (Yang & Wang, 2020) into an optimal control model and analyzed. For the extended optimal control model, we preformed numerical simulations using an iterative fourth-order Runge-Kutta integration scheme to support

the analytical results. Secondly, we developed a mathematical model which describe the dynamics of COVID-19 using the system of non-linear ordinary differential equations. We then show that the proposed mathematical model is well-posed in a biologically feasible domains. We then studied the formulated governing mathematical model analytically to understand the physical meaning of the governing equation. Both local and global stability analysis of the equilibrium points of the model equations is investigated using the Jacobian matrix and via appropriate Lyapunov functions, respectively. The analytical solutions of the model equations was supplemented by numerical simulations by appropriately choosing (and estimating) the system parameter values using MATLAB.

CHAPTER 4

OPTIMAL CONTROL STRATEGIES FOR THE TRANSMISSION RISK OF COVID-19

4.1 COVID-19 model with controls

In this section, we consider a mathematical model proposed in (Yang & Wang, 2020) to study the transmission dynamics of novel coronavirus epidemic. In the model, we introduce three control functions $u_1(\cdot)$, $u_2(\cdot)$ and $u_3(\cdot)$. The first control u_1 represents preventive measures such as quarantine, and isolation that help to reduce contact rate. The control u_2 represents intense medical care for all the confirmed cases to increase recover rate of infected individuals and the control u_3 measures the effort made to reduce the concentration of coronavirus from the environmental reservoir through surface disinfection procedures. The governing mathematical model is expressed by the following system of nonlinear ordinary differential equations:

$$\begin{aligned}
\frac{dS}{dt} &= \Lambda - (1-u_1(t))\left(\beta_E(E)SE + \beta_I(I)SI + \beta_V(V)SV\right) - \mu S,\\
\frac{dE}{dt} &= (1-u_1(t))\left(\beta_E(E)SE + \beta_I(I)SI + \beta_V(V)SV\right) - (\alpha+\mu)E,\\
\frac{dI}{dt} &= \alpha E - (w+\gamma+u_2(t)+\mu)I,\\
\frac{dR}{dt} &= (u_2(t)+\gamma)I - \mu R,\\
\frac{dV}{dt} &= \xi_1 E + \xi_2 I - (\sigma+u_3(t))V.
\end{aligned} \tag{4.1}$$

We assume that the initial conditions

$$S(0) > 0,\ E(0) \geq 0,\ I(0) \geq 0,\ R(0) \geq 0,\ V(0) \geq 0 \tag{4.2}$$

of the governing control systems are non-negative. The control system (4.1) involves five state variables: Susceptible $S(t)$, exposed $E(t)$, infected $I(t)$, recovered $R(t)$ and V is the concentration of the coronavirus in the environmental reservoir for all $t \geq 0$.

We adopt other important assumption and descriptions from (Yang & Wang, 2020). Individuals in the infected class have fully developed disease symptoms and can infect other people. Individuals in the exposed class are in the incubation period and they are asymptomatic but still capable of infecting others.The parameter Λ represents the population influx, μ is the natural death rate of human hosts, α^{-1} is the incubation period between the infection and the onset of symptoms, w is the disease-induced death rate, γ is the rate of recovery from infection, ξ_1 and ξ_2 are the respective rates of the exposed and infected individuals contributing the coronavirus to the environmental reservoir, and σ is the removal rate of the virus from the environment.The functions

$\beta_E(E)$ and $\beta_I(I)$ represent the direct,human-to-human transmission rates between the exposed and susceptible individuals, and between infected and susceptible individuals, respectively. The model involves human population and hence all the parameters used are non-negative. The function $\beta_V(V)$ represents the indirect, environment-to- human transmission rate. In particular, we assume that $\beta_E(E)$, $\beta_I(I)$ and $\beta_V(V)$ are all non-increasing functions, given that higher values of E, I and V would motivate stronger control measures that could reduce the transmission rates. More precisely, the following assumptions hold:

(1) All $\beta_E(E)$, $\beta_I(I)$ and $\beta_V(V)$ are positive; and

(2) $\beta_E'(E) \leq 0$, $\beta_I'(I) \leq 0$ and $\beta_V'(V) \leq 0$.

In numerical simulation, the authors used the following functions for the three transmission rates in their model:

$$\beta_E(E) = \frac{\beta_{E0}}{1+cE}, \qquad \beta_I(I) = \frac{\beta_{I0}}{1+cI}, \qquad \beta_V(V) = \frac{\beta_{V0}}{1+cV} \tag{4.3}$$

where β_{E0}, β_{I0} and β_{V0} are all positive constants denoting the maximum values of these transmission rates. The parameter c is a positive coefficient providing adjustment to the transmission rates. The values of model parameter depicted in Table 4.1 are taken from (Yang & Wang, 2020).

Table 4.1: Values of model parameters.

Parameter	Description	Value
Λ	Influx rate	271.23 per day
β_{E0}	Transmission constant between S and E	3.11×10^{-8} /person/day
β_{I0}	Transmission constant between S and I	0.62×10^{-8} /person/day
β_{V0}	Transmission constant between S and V	1.03×10^{-8}
μ	Natural death rate	3.01×10^{-5} per day
c	Transmission adjustment coefficient	1.01×10^{-4}
ξ_1	Virus shedding rate by exposed people	2.30
ξ_2	Virus shedding rate by infected people	0 per person per day per ml
α^{-1}	Incubation period	7 days
w	Disease-induced death rate	0.01 per day
γ	Recovery rate	1/15 per day
σ	Removal rate of virus	1 per day

Without controls, the basic reproduction number $\mathcal{R}_0$ for system (4.1) is given by

$$\mathcal{R}_0 = \left[\frac{\beta_E(0)}{\alpha+\mu} + \frac{\beta_I(0)\,\alpha}{(\alpha+\mu)\,\psi} + \frac{\beta_V(0)\,(\xi_1+\xi_1\psi+\xi_2\alpha)}{(\alpha+\mu)\,\psi\sigma}\right]\frac{\Lambda}{\mu}. \tag{4.4}$$

The basic reproduction number $\mathcal{R}_0$ play fundamental role in disease modelling and is defined as the average number of new infected cases produced by a single infectious individual introduced in a totally susceptible population (Area et al., 2017; Hethcote, 2000; Khan et al., 2019). Basically, it is used to predict the global dynamics of the disease whether the disease is controllable or not. In the following result, we compute the basic reproduction number $\mathcal{R}_0$ of the system (4.1) using next generation matrix method introduced in (Van den Driessche & Watmough, 2002).

Proposition 1. *The basic reproduction number $\mathcal{R}_0$ for system (4.1) is given by*

$$\mathcal{R}_0(u_1,u_2,u_3) = \left[\frac{\beta_E(0)}{\alpha+\mu} + \frac{\beta_I(0)\,\alpha}{(\alpha+\mu)\,(\psi+u_2)} + \frac{\beta_V(0)\,(\xi_1 u_2+\xi_1\psi+\xi_2\alpha)}{(\alpha+\mu)\,(\psi+u_2)\,(\sigma+u_3)}\right]\frac{(1-u_1)\Lambda}{\mu} \tag{4.5}$$

Proof. The disease free equilibrium solution with $E = I = 0$ of system (4.1) is given by

$$\bar{E} = (S_0, E_0, I_0, R_0, V_0) = \left(\frac{\Lambda}{\mu}, 0, 0, 0, 0\right), \tag{4.6}$$

and its stability is obtained in (Yang & Wang, 2020). We calculate the basic reproduction number $\mathcal{R}_0(u_1,u_2,u_3)$ using the method detailed in (Van den Driessche & Watmough, 2002). For this, we write the right-hand side of system (4.1) as $\mathcal{F}-\mathcal{V}$ with

$$\mathcal{F} = \begin{bmatrix}(1-u_1(t))\,(\beta_E(E)SE+\beta_I(I)SI+\beta_V(V)SV)\\ 0\\ 0\end{bmatrix},\ \mathcal{V} = \begin{bmatrix}(\alpha+\mu)E\\ -\alpha E+(w+\gamma+u_2(t)+\mu)I\\ -\xi_1 E-\xi_2 I+(\sigma+u_3(t))V\end{bmatrix}.$$

The $\mathcal{F}_i$ entry denotes the rate of appearance of new infections in compartment i, and $\mathcal{V}_i$ also denotes the rate of other transitions between compartment i and other infected compartments. Next we compute the Jacobian F associated with $\mathcal{F}$ and evaluate at equilibrium solution to obtain

$$\mathrm{F}(\bar{E}) = \begin{bmatrix}(1-u_1)\,\beta_E(0)\,S_0 & (1-u_1)\,\beta_I(0)\,S_0 & (1-u_1)\,\beta_V(0)\,S_0\\ 0 & 0 & 0\\ 0 & 0 & 0\end{bmatrix}$$

and similarly the Jacobian V associated with $\mathcal{V}$ given by

$$V = \begin{bmatrix} \alpha+\mu & 0 & 0 \\ -\alpha & \psi+u_2 & 0 \\ -\xi_1 & -\xi_2 & \sigma+u_3 \end{bmatrix}.$$

From the biological and mathematical meanings of F and V, it follows that F is entrywise non-negative and V is a non-singular M-matrix.Thus, the inverse of matrix V exists and given by

$$\mathrm{V}^{-1} = \begin{bmatrix} (\alpha+\mu)^{-1} & 0 & 0 \\ \frac{\alpha}{(\alpha+\mu)(\psi+u_2)} & (\psi+u_2)^{-1} & 0 \\ \frac{\alpha\xi_2+\xi_1 u_2+\xi_1\psi}{(\alpha+\mu)(\psi+u_2)(\sigma+u_3)} & \frac{\xi_2}{(\psi+u_2)(\sigma+u_3)} & (\sigma+u_3)^{-1} \end{bmatrix}$$

where $\psi = w+\gamma+\mu$. Hence, the basic reproduction number can then be computed as $\mathcal{R}_0 = \rho(\mathrm{FV}^{-1})$ which is the spectral radius of the matrix and given as in(4.5). Note, if we denote the number of initially infected individuals with novel coronavirus by $\phi(0)$, then $\mathrm{FV}^{-1}\phi(0)$ is an entry-wise non-negative vector giving the expected number of new infections. Further, the (i,j) entry of the next generation matrix FV^{-1} is the expected number of new infections in compartment i produced by the infected individual originally introduced into compartment j assuming that the environment seen by the individual remains homogeneous for the duration of its infection. This complete the proof. □

In (4.5) $\frac{\beta_E(0)\Lambda(1-u_1)}{\mu(\alpha+\mu)}$ control the disease transmission from exposed human-to-susceptible human and the second term $\frac{\alpha\beta_I(0)\Lambda(1-u_1)}{\mu(\alpha+\mu)(\psi+u_2)}$ influence the disease transmission from infected human-to-susceptible human. The last term, $\frac{\beta_V(0)\,(\xi_1 u_2+\xi_1\psi+\xi_2\alpha)\Lambda(1-u_1)}{\mu(\alpha+\mu)(\psi+u_2)(\sigma+u_3)}$ control the disease transmission from environment-to-susceptible human.These control measures are assumed to influence the dynamics of COVID-19 outbreak. Also note that for $u_1 = u_2 = u_3 = 0$,i.e.,in the absence of control functions the governing system (4.1) and the basic reproduction numbers(4.5) are respectively reduced to the model and reproduction number proposed in (Yang & Wang, 2020). Now onwards, we consider $\beta_E(0) = \beta_E$, $\beta_I(0) = \beta_I$, and $\beta_V(0) = \beta_V$ for our convenience.

4.1.1 Sensitivity of basic reproduction number ($\mathcal{R}_0$)

In this subsection, we analyse the effect of different model parameters to specify the comparative impact of these parameters in the disease transmission. For this, we need to compute the partial derivative of $\mathcal{R}_0$ with respect to model parameters. For instance, a direct calculation shows that $\frac{\partial\mathcal{R}_0}{\partial u_i} \leq 0,\ i = 1,2,3$ for all values of the model parameters. This implies that the basic reproduction number decreases with respect to u_1, u_2 and u_3 respectively. Table 4.2 shows the

sensitivity indices of $\mathcal{R}_0$ to the parameters for the novel coronavirus model described in(4.1).

Table 4.2: Sensitivity indices for model parameters.

Parameter	Description	Sensitivity indices
Λ	Influx rate	+ve
β_E	Transmission constant between S and E	+ve
β_I	Transmission constant between S and I	+ve
β_V	Transmission constant between S and V	+ve
ξ_1	Virus shedding rate by exposed people	+ve
ξ_2	Virus shedding rate by infected people	+ve
μ	Natural death rate	-ve
α^{-1}	Incubation period	-ve
w	Disease-induced death rate	-ve
γ	Recovery rate	-ve
σ	Removal rate of virus	-ve

The sensitivity of the basic reproduction number is a crucial tool to determine the model robustness to parameter values. If $\mathcal{R}_0$ is a differentiable function of the parameter, the sensitivity index can alternatively defined using partial derivatives as in Definition1.

Definition 1. *(Chitnis et al., 2008) The normalized forward sensitivity index of $\mathcal{R}_0$, that depends differentiably on a parameter, p, is defined as:*

$$\Psi_p^{\mathcal{R}_0} := \frac{\partial \mathcal{R}_0}{\partial p} \times \frac{p}{\mathcal{R}_0}. \tag{4.7}$$

From this definition we can deduce that the sensitivity indices are useful to measure the relative change in a state variable when a parameter changes. Now, we calculate the sensitivity indices of $\mathcal{R}_0$ with respect to model parameters using (4.7).

$$\Psi_{\Lambda}^{\mathcal{R}_0} = \frac{\partial \mathcal{R}_0}{\partial \Lambda} \times \frac{\Lambda}{\mathcal{R}_0} = 1, \quad \Psi_{u_1}^{\mathcal{R}_0} = \frac{\partial \mathcal{R}_0}{\partial u_1} \times \frac{u_1}{\mathcal{R}_0} = \frac{u_1}{u_1 - 1} < 0,$$
$$\Psi_{u_2}^{\mathcal{R}_0} = \frac{\partial \mathcal{R}_0}{\partial u_2} \times \frac{u_2}{\mathcal{R}_0} = \frac{-\alpha(\xi_2\beta_V + \beta_I(\sigma+u_3))u_2}{(w+\gamma+\mu+u_2)(\beta_E(w+\gamma+\mu+u_2)(\sigma+u_3)+((w+\gamma+\mu+u_2)\xi_1+\xi_2\alpha)\beta_V+\beta_I\alpha(\sigma+u_3))} < 0,$$
$$\Psi_{u_3}^{\mathcal{R}_0} = \frac{\partial \mathcal{R}_0}{\partial u_3} \times \frac{u_3}{\mathcal{R}_0} = \frac{-(1-u_1)\beta_V(\xi_1 u_2+\xi_1(w+\gamma+\mu)+\xi_2\alpha)u_3}{(\sigma+u_3)(\beta_E(w+\gamma+\mu+u_2)(\sigma+u_3)+((w+\gamma+\mu+u_2)\xi_1+\xi_2\alpha)\beta_V+\beta_I\alpha(\sigma+u_3))(u_1-1)} < 0,$$
$$\Psi_{\beta_E}^{\mathcal{R}_0} = \frac{\partial \mathcal{R}_0}{\partial \beta_E} \times \frac{\beta_E}{\mathcal{R}_0} = \frac{(1-u_1)(w+\gamma+\mu+u_2)(\sigma+u_3)\beta_E}{(\beta_E(w+\gamma+\mu+u_2)(\sigma+u_3)+((w+\gamma+\mu+u_2)\xi_1+\xi_2\alpha)\beta_V+\beta_I\alpha(\sigma+u_3))(1-u_1)} > 0,$$
$$\Psi_{\beta_I}^{\mathcal{R}_0} = \frac{\partial \mathcal{R}_0}{\partial \beta_I} \times \frac{\beta_I}{\mathcal{R}_0} = \frac{(1-u_1)\alpha(\sigma+u_3)\beta_I}{(\beta_E(w+\gamma+\mu+u_2)(\sigma+u_3)+((w+\gamma+\mu+u_2)\xi_1+\xi_2\alpha)\beta_V+\beta_I\alpha(\sigma+u_3))(1-u_1)} > 0,$$
$$\Psi_{\beta_V}^{\mathcal{R}_0} = \frac{\partial \mathcal{R}_0}{\partial \beta_V} \times \frac{\beta_V}{\mathcal{R}_0} = \frac{(1-u_1)(\xi_1 u_2+\xi_1(w+\gamma+\mu)+\xi_2\alpha)\beta_V}{(\beta_E(w+\gamma+\mu+u_2)(\sigma+u_3)+((w+\gamma+\mu+u_2)\xi_1+\xi_2\alpha)\beta_V+\beta_I\alpha(\sigma+u_3))(1-u_1)} > 0,$$
$$\Psi_{\gamma}^{\mathcal{R}_0} = \frac{\partial \mathcal{R}_0}{\partial \gamma} \times \frac{\gamma}{\mathcal{R}_0} = \frac{-\alpha(\xi_2\beta_V+\beta_I(\sigma+u_3))\gamma}{(w+\gamma+\mu+u_2)(\beta_E(w+\gamma+\mu+u_2)(\sigma+u_3)+((w+\gamma+\mu+u_2)\xi_1+\xi_2\alpha)\beta_V+\beta_I\alpha(\sigma+u_3))} < 0,$$
$$\Psi_{\sigma}^{\mathcal{R}_0} = \frac{\partial \mathcal{R}_0}{\partial \sigma} \times \frac{\sigma}{\mathcal{R}_0} = \frac{-(1-u_1)\beta_V(\xi_1 u_2+\xi_1(w+\gamma+\mu)+\xi_2\alpha)\sigma}{(\sigma+u_3)(\beta_E(w+\gamma+\mu+u_2)(\sigma+u_3)+((w+\gamma+\mu+u_2)\xi_1+\xi_2\alpha)\beta_V+\beta_I\alpha(\sigma+u_3))(u_1-1)} < 0,$$

$$\Psi_{\xi_1}^{\mathcal{R}_0} = \frac{\partial \mathcal{R}_0}{\partial \xi_1} \times \frac{\xi_1}{\mathcal{R}_0} = \frac{(1-u_1)\beta_V\,(w+\gamma+\mu+u_2)\xi_1}{(\beta_E\,(w+\gamma+\mu+u_2)(\sigma+u_3)+((w+\gamma+\mu+u_2)\xi_1+\xi_2\,\alpha)\beta_V+\beta_I\,\alpha\,(\sigma+u_3))(1-u_1)} > 0,$$
$$\Psi_{\xi_2}^{\mathcal{R}_0} = \frac{\partial \mathcal{R}_0}{\partial \xi_2} \times \frac{\xi_2}{\mathcal{R}_0} = \frac{(1-u_1)\beta_V\,\alpha\xi_2}{(\beta_E\,(w+\gamma+\mu+u_2)(\sigma+u_3)+((w+\gamma+\mu+u_2)\xi_1+\xi_2\,\alpha)\beta_V+\beta_I\,\alpha\,(\sigma+u_3))(1-u_1)} > 0.$$

We derived an analytical expression for the sensitivity of $\mathcal{R}_0$, $\Psi_p^{\mathcal{R}_0} = \frac{\partial \mathcal{R}_0}{\partial p} \times \frac{p}{\mathcal{R}_0}$, with respect to various model parameters. From Table 4.2 we can see that parameters $\beta_E, \beta_I, \beta_V, \xi_1, \xi_2$ and Λ have a positive sign which means that $\mathcal{R}_0$ increases with the parameter. While the rest of parameters have negative sign means that $\mathcal{R}_0$ decreases for higher values of the parameters. Further, this implies that by increasing (or decreasing) of p by $\chi\%$ will increase(or decrease) the basic reproduction number by $\chi\%$. In the study of sensitivity analysis, it is not ethically acceptable increasing human mortality rate to control disease epidemic and hence do not considered.

4.2 The optimal control problem

In this section, we analyse an optimal control problem describing the mitigations of COVID-19 outbreak. The objective is to find the optimal values $\bar{u} = (\bar{u}_1, \bar{u}_2, \bar{u}_3)$ of the controls $u = (u_1, u_2, u_3)$ such that the associated state trajectories $\bar{S}$, $\bar{E}$, $\bar{I}$, $\bar{R}$, $\bar{V}$ are solution of the system (4.1) in the intervention time interval $[0, T]$ with initial conditions as given in (4.2) and minimize the objective functional. The control function u_1 play the role of preventive measures including: social distance, tracing patient, quarantine and isolation that help to reduce contact rate with health individuals. The control u_2 represents intense medical care for all the confirmed cases to increase recover rate of infected individuals while the control function u_3 measure the effort made to reduce the concentration of coronavirus from the environmental reservoir through surface disinfection procedures.The controls are bounded between 0 and 1. When the controls vanish, it means no extra measures are implemented for the reduction of the disease. When the controls take the maximum value 1, it means that the intervention is 100 % perfectly implemented which is not true in reality and thus we assumed $u_i \leq 1-\varepsilon, i = 1,2,3$, where $\varepsilon \ll 1$ denotes a positive real number.

Our cost functional considers the number of exposed individuals E, the number of infected individuals I, and the implementation cost of strategies related to the controls $u_i,\ i = 1,2,3$. More precisely, the objective functional is given by

$$J[u_1, u_2, u_3] = \int_0^T \left(C_1 E(t) + C_2 I(t) + \frac{1}{2}\sum_{i=1}^{3} B_i u_i^2 \right) dt \to min \tag{4.8}$$

where constants C_1, C_2 and B_i are positive. The weight constants B_1,B_2 and B_3 are the measure of relative costs of interventions associated with the controls u_1, u_2 and u_3, respectively and also balances the units of integrand. In the cost functional, the term $C_1 E(t)$ describe the cost related to asymptomatic class while $C_2 I(t)$ denotes the cost incurred due to symptomatic compartment. Additionally, the functional J corresponds the total cost due to coronavirus outbreak and its control

strategies. Further, the integrand function $L(S,E,I,R,V,u_1,u_2,u_3) = C_1I(t) + C_2E(t) + \frac{1}{2}\sum_{i=1}^{3} B_i u_i^2$ measures the current cost at time t. Lastly, the fixed constant T denotes the terminal innervation time.

The set of admissible control functions is defined by

$$\Omega_\varepsilon = \{(u_1(\cdot),u_2(\cdot),u_3(\cdot)) \in (Ł^\infty(0,T))^3 : 0 \le u_1(t),u_2(t),u_3(t) \le 1-\varepsilon, \forall t \in [0,T]\}. \quad (4.9)$$

Then we consider the optimal control problem of obtaining $(\bar{S},(\cdot),\bar{E}(\cdot),\bar{I}(\cdot),\bar{R}(\cdot),\bar{V}(\cdot))$, associated with an admissible control triple $(\bar{u}_1(\cdot),\bar{u}_2(\cdot),\bar{u}_3(\cdot)) \in \Omega_\varepsilon$ on the intervention time interval $[0,T]$, subjected to the state system (4.1) in $\mathbb{R}^5$ with initial condition given in (4.2) and minimizing the cost functional (4.8). More precisely, the optimal control problem can be defined as

$$J[\bar{u}_1,\bar{u}_2,\bar{u}_3] = \min_{\Omega_\varepsilon} J[u_1(\cdot),u_2(\cdot),u_3(\cdot)] \quad (4.10)$$

satisfying (4.1) and (4.2).

4.2.1 Existence of optimal controls

In this subsection, we prove the existence of such optimal control functions which minimize the cost function in the finite intervention period. The following result guarantees the existence of optimal control functions. A detail and similar analysis on existence of optimal control can be found in(Fleming & Rishel, 2012; Kumar et al., 2020; Silva & Torres, 2013).

Theorem 2. *There exists an optimal control triple $\bar{u} = (\bar{u}_1,\bar{u}_2,\bar{u}_3)$ in Ω_ε and a corresponding solution vector $\bar{X} = \left(\bar{S},\bar{E},\bar{I},\bar{R},\bar{V}\right)$ to the initial value problem (4.1)-(4.2) such that*

$$J[\bar{u}_1,\bar{u}_2,\bar{u}_3] = \min_{\Omega_\varepsilon} J[u_1(\cdot),u_2(\cdot),u_3(\cdot)] \quad (4.11)$$

Proof. All the state variable involved in the model are continuously differentiable. Therefore, we need to verify the following four conditions given in (Fleming & Rishel, 2012).

(i) the set of solutions to the system (4.1)-(4.2) with control variables in (4.9) are nonempty.

(ii) the set Ω_ε is convex and closed.

(iii) the state system can be written as linear function of control variables with coefficients depending on time and state variables.

(iv) the integrand L of (4.8) is convex on Ω_ε and $L(S,E,I,R,V,u) \ge g(u)$, where g is continuous and $||u||^{-1}g(u) \to +\infty$ as $||u|| \to \infty$.

Note that all the state variables $S,E,I,R \in C(\mathbb{R}^+,\mathbb{R}^+)$ and the total human population is defined as

$$N = S(t)+E(t)+I(t)+R(t).$$

From governing system (4.1) it follows that

$$\frac{dN}{dt} = \Lambda - wI - \mu N \leq \Lambda - \mu N.$$

From this it follows that $\limsup_{t\to\infty} N(t) \leq \frac{\Lambda}{\mu}$. Further, the concentration of coronavirus in the environmental reservoir is given by

$$\frac{dV}{dt} = \xi_1 E + \xi_2 I - (\sigma + u_3(t))V \leq \xi_1 E + \xi_2 I - \sigma V.$$

This gives also that $\limsup_{t\to\infty} V(t) \leq \frac{\Lambda}{\mu}(\xi_1+\xi_2)$. From which it follows that the solutions of the state system are continuous and bounded for each admissible control functions in Ω_ε. Further, the right hand side functions of the model equations (4.1) satisfies the Lipschitz condition with respect to state variables. Therefore, the initial vale problem (4.1) -(4.2) has a unique solution corresponding to each admissible control function $u \in \Omega_\varepsilon$(Coddington & Levinson, 1955). Thus, condition (i) is proved.

To prove (ii), consider

$$\Omega_\varepsilon = \{u \in \mathbb{R}^3 : ||u|| \leq 1-\varepsilon\}.$$

Let $u_1,u_2 \in \Omega_\varepsilon$ such that $||u_1|| \leq 1-\varepsilon$ and $||u_2|| \leq 1-\varepsilon$. Then for any $\rho \in [0,1]$,

$$||\rho u_1 + (1-\rho)u_2|| \leq \rho||u_1|| + (1-\rho)||u_2|| \leq 1-\varepsilon.$$

This implies that Ω is convex and closed.

The state system (4.1) is clearly linear in control variables u_1,u_2 and u_3 with coefficients depending on state variables. With this condition (iii) is satisfied. The integrand of the cost functional $L(S,E,I,R,V,u) = C_1I(t)+C_2E(t)+\frac{1}{2}\sum_{i=1}^{3} B_iu_i^2$ is the sum of convex function and hence convex with respect to control variables. Furthermore,

$$L(S,E,I,R,V,u) = C_1I(t)+C_2E(t)+\frac{1}{2}\sum_{i=1}^{3} B_iu_i^2 \geq \frac{1}{2}\sum_{i=1}^{3} B_iu_i^2. \tag{4.12}$$

Let $\eta = \min(\frac{B_1}{2},\frac{B_2}{2},\frac{B_3}{2}) > 0$ and define a continuous function $g(u) = \eta||u||^2$. Then from equation(4.12) we have $L(S,E,I,R,V,u) \geq g(u)$. Clearly $||u||^{-1}g(u) \to +\infty$ as $||u|| \to \infty$. Thus, condition (iv) is achieved. Therefore, the existence of an optimal control pair $(\bar{X},\bar{u})$ satisfying (4.1)-(4.2) and (4.11)is assured by results given in (Fleming & Rishel, 2012). The proof is completed. □

4.2.2 Characterization of optimal control

In this section, we present optimality conditions for the optimal control problem defined above and detail its properties. According to Pontryagin's Minimum Principle(Lemos-Paião et al., 2017; Pontryagin et al., 2018), if $\bar{u}(\cdot) \in \Omega_\varepsilon$ is optimal for problem (4.1)-(4.2) and (4.10) with fixed final time T, then there exists a non-trivial absolutely continuous mapping $\lambda : [0,T] \to \mathbb{R}^5, \lambda = (\lambda_1(t), \lambda_2(t), \lambda_3(t), \lambda_4(t), \lambda_5(t))$ called the adjoint vector, such that

1. the Hamiltonian function is defined as

$$\mathcal{H} = C_1 I(t) + C_2 E(t) + \frac{1}{2}\sum_{i=1}^{3} B_i u_i^2 + \sum_{i=1}^{5} \lambda_i(t) g_i(t,S,E,I,R,V,u), \tag{4.13}$$

   where g_i stands for the right hands of the constraints (4.1) for $i = 1, 2, 3, 4, 5$.

2. the control system

$$S' = \frac{\partial \mathcal{H}}{\partial \lambda_1}, \quad E' = \frac{\partial \mathcal{H}}{\partial \lambda_2}, \quad I' = \frac{\partial \mathcal{H}}{\partial \lambda_3}, \quad R' = \frac{\partial \mathcal{H}}{\partial \lambda_4}, \quad V' = \frac{\partial \mathcal{H}}{\partial \lambda_5}; \tag{4.14}$$

3. the adjoint system

$$\lambda_1' = -\frac{\partial \mathcal{H}}{\partial S}, \quad \lambda_2' = -\frac{\partial \mathcal{H}}{\partial E}, \quad \lambda_3' = -\frac{\partial \mathcal{H}}{\partial I}, \quad \lambda_4' = -\frac{\partial \mathcal{H}}{\partial R}, \quad \lambda_5' = -\frac{\partial \mathcal{H}}{\partial V}; \tag{4.15}$$

4. and the optimality condition

$$\mathcal{H}(\bar{S}(t), \bar{E}(t), \bar{I}(t), \bar{R}(t), \bar{V}(t), \bar{u}(t), \bar{\lambda}(t)) = \min_{u \in \Omega_\varepsilon} \mathcal{H}(\bar{S}(t), \bar{E}(t), \bar{I}(t), \bar{R}(t), \bar{V}(t), u(t), \bar{\lambda}(t)) \tag{4.16}$$

   holds for almost all $t \in [0,T]$.

5. Moreover, the transversality condition

$$\lambda_i(T) = 0, \qquad i = 1, \ldots, 5 \tag{4.17}$$

   also holds true.

In the next result, we discuss characterization of optimal controls and adjoint variables.

Theorem 3. *Let $\bar{u} = (\bar{u}_1, \bar{u}_2, \bar{u}_3)$ be the optimal control and $(\bar{S}(\cdot), \bar{E}(\cdot), \bar{I}(\cdot), \bar{R}(\cdot), \bar{V}(\cdot))$ be the associated unique optimal solutions of the optimal control problem (4.1)-(4.2) and (4.8)-(4.9) with fixed final time T. Then there exists adjoint function $\bar{\lambda}_i(\cdot), i = 1, \ldots, 5$ satisfying the following*

canonical equations:

$$\begin{cases} \lambda_1^{'} &= (1-u_1)\left(\frac{\beta_{E^0} E}{cE+1}+\frac{\beta_{I^0} I}{cI+1}+\frac{\beta_{V^0} V}{cV+1}\right)(\lambda_1-\lambda_2)+\lambda_1\mu, \\ \lambda_2^{'} &= -C_2+(1-u_1)\left(\frac{\beta_{E^0} S}{cE+1}-\frac{\beta_{E^0} cSE}{(cE+1)^2}\right)(\lambda_1-\lambda_2)+\lambda_2(\alpha+\mu)-\lambda_3\alpha-\lambda_5\xi_1, \\ \lambda_3^{'} &= -C_1+(1-u_1)\left(\frac{\beta_{I^0} S}{cI+1}-\frac{\beta_{I^0} cSI}{(cI+1)^2}\right)(\lambda_1-\lambda_2)+\lambda_3(w+\gamma+u_2+\mu)-\lambda_4(u_2+\gamma)-\lambda_5\xi_2, \\ \lambda_4^{'} &= \mu\lambda_4 \\ \lambda_5^{'} &= (1-u_1)\left(\frac{\beta_{V^0} S}{cV+1}-\frac{\beta_{V^0} cSV}{(cV+1)^2}\right)(\lambda_1-\lambda_2)+\lambda_5(\sigma+u_3). \end{cases} \tag{4.18}$$

with transiversality conditions

$$\bar{\lambda}_i(T)=0, \qquad i=1,\ldots,5. \tag{4.19}$$

Moreover, the corresponding optimal controls $\bar{u}_1(t),\bar{u}_2(t)$ and $\bar{u}_3(t)$ are given by

$$\bar{u}_1(t)=\min\left\{\max\left\{0,\frac{\lambda_2-\lambda_1}{B_1}\left(\frac{\beta_{E^0} SE}{cE+1}+\frac{\beta_{I^0} SI}{cI+1}+\frac{\beta_{V^0} SV}{cV+1}\right)\right\},1-\varepsilon\right\}, \tag{4.20}$$

$$\bar{u}_2(t)=\min\left\{\max\left\{0,\frac{(\lambda_3-\lambda_4)I}{B_2}\right\},1-\varepsilon\right\}, \qquad \bar{u}_3(t)=\min\left\{\max\left\{0,\frac{\lambda_5 V}{B_3}\right\},1-\varepsilon\right\}. \tag{4.21}$$

Proof. The adjoint system, transversality conditions and optimality conditions are standard results from Pontryagin's Minimum Principle (Lemos-Paião et al., 2017; Pontryagin et al., 2018). Thus, system (4.18) is directly derived from (4.15) and the transversality conditions (4.19) follows from(4.17). Further, using the optimality condition it follows that

$$\frac{\partial H}{\partial u_i}=0, \text{ for } i=1,2,3. \tag{4.22}$$

Consequently, the optimal controls (4.20)-(4.21) can be directly solved from (4.22) by taking into account the boundedness condition given in (4.9). □

4.3 Numerical simulations

In this section, we study numerically the solution of the optimal control problem proposed in Section (4.1) and explain the impact of control strategies on the spread of coronavirus outbreak. For this purpose, we apply the forward-backward sweep method presented in the book of (Lenhart & Workman, 2007).

To briefly summarize the procedure, first we solve the control system with an initial guess

for the control variables using forward fourth-order Runge-Kutta scheme and transversality conditions. The adjoint system is then solved applying the backward fourth-order Runge-Kutta scheme using the current solution of state variables. Then, the controls are updated by means of convex combination of the previous controls and the values computed in the characterizations process. The updated controls are then utilized to repeat the solution of state and adjoint systems. The iteration continued until a predefined convergence criterion is met.
To illustrate the numerical results, we use the COVID-19 outbreak real data and the initial conditions

$$(S(0),E(0),I(0),R(0),V(0)) = (8998505,1000,475,10,10000)$$

reported in (Yang & Wang, 2020) as given in Table 4.1. The data, basically covers the epidemic period from January 23, 2020 to February 10, 2020, when the city of Wuhan was placed in quarantine.

Fist, we compare the number of exposed and infectious population with and without controls. For this, we consider $C_1 = 0.25$, $C_2 = 0.7$, $B_1 = 8$, $B_2 = 290$, $B_3 = 65$ and final intervention time $T = 300$ days. We also choose $\varepsilon = 0.05$ to restrict the maximum values of control variables.

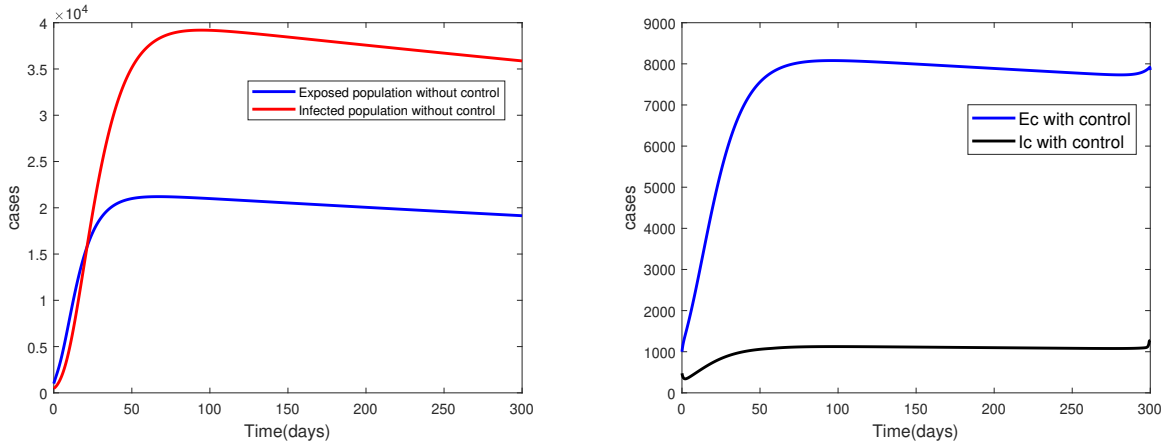

(a) Exposed and infected populations without control. (b) Exposed and infected populations with control.

Figure 4.1: Simulation results comparing the size of COVID-19 outbreak in Wuhan City with and without optimal control.

In Fig.4.1 we observe that the implementation of maximum prevention (quarantine, isolation, social distancing), intensive medical care and surface disinfection all together have significant impact on the reduction of the exposed and infectious populations and disease prevalence. The result plotted in Fig.1(a) shows good agreement with result obtained in (Yang & Wang, 2020).The profiles of corresponding optimal controls representing: preventive measures u_1, intensive medical care u_2 and surface disinfection u_3 are plotted in Fig.4.2.

Remark 1. *Note that the value of co-state functions are zero at time $T = 300$ days and consequently, all the control variables are vanished at this time. For these parameter values the*

reproduction number completely damped below one except at the terminal time.

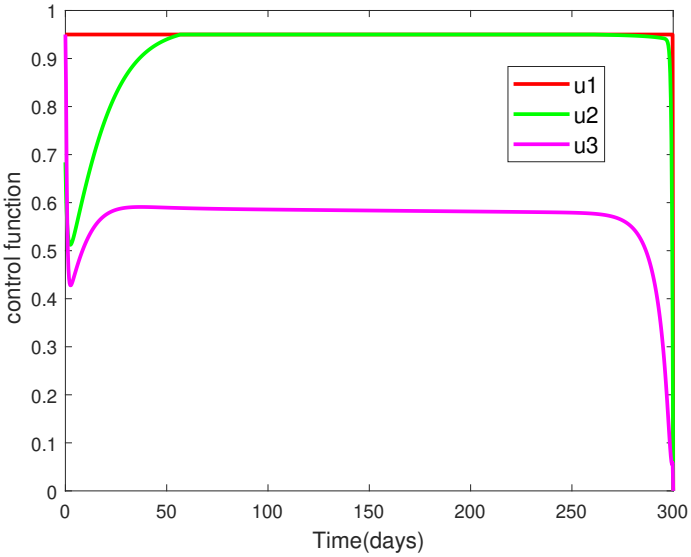

Figure 4.2: Profiles of optimal control function u_1, u_2 and u_3.

In the following, we comparatively analyse the impact of control strategies on the spread of disease under different combinations of scenarios:

i. Applying medical care $u_2 \neq 0$ and surface disinfection $u_3 \neq 0$ without prevention$u_1 = 0$,

ii. Intensive prevention u_1^{max} with medical care $u_2 \neq 0$, and

iii. Intensive implementation of prevention $u_1^{\max}$, medical care $u_2^{\max}$ and surface disinfection $u_3^{\max}$.

In the first case, we preform simulation of control system in the absence of $u_1 = 0$. For this, we assign the positive constants $C_1 = 0.12$, $C_2 = 0.4$, $B_1 = 650$ and $B_3 = 550$ with initial population as given above.The values of the remaining model parameters are as presented in Table4.1. The aim of this case is to investigate the impact of intensive medical care and surface disinfection on the disease spread without prevention. The matching numerical results are displayed in Fig. 4.3. From this figure, one can observe that the exposed populations are about 17,000 and the infective populations are nearly 2000 at final time. Here, the applied strategy seems effective in reducing the disease burden within the intervention period and thus can be consider as optimal candidate to manage the burden of COVID-19 infection.

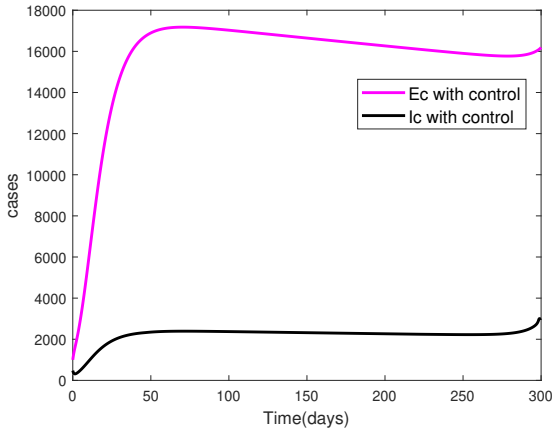

(a) Exposed and infected populations with control .

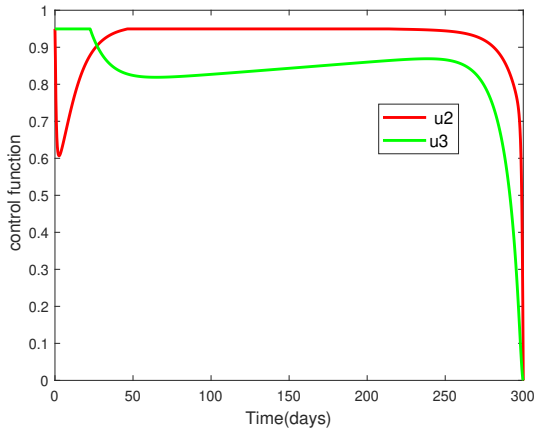

(b) Profile of control functions u_2 and u_3 .

Figure 4.3: A simulation result in the absence of intensive prevention.

Now, to understand in detail, we plotted the corresponding basic reproduction number $\mathcal{R}_0$ in the absence of control $u_1 = 0$ using(4.5) and explored indirectly the effectiveness of these control strategies. Fig.4.4 displays the profile of $\mathcal{R}_0$ in the absence of u_1. Note that the values of different parameter changes the magnitude of $\mathcal{R}_0$ and thus ultimately reflect the severity of disease outbreak. Clearly, one can observe from Fig.4.4 that the basic reproduction number still greater than one. Thus, the combined effect of both intensive medical care and surface disinfection are relatively reduced exposed and infected population without showing strong decrease in disease incidence. Hence, we deduce that strategy (i) is not be preferable since the value of the reproduction number is higher than one.

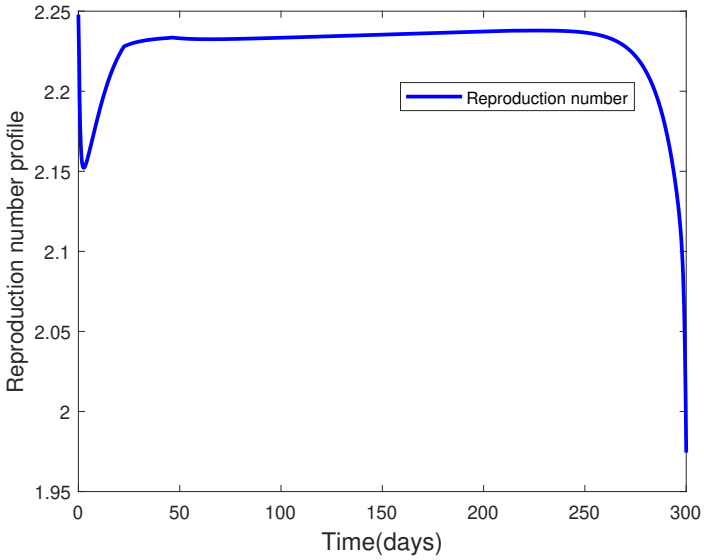

Figure 4.4: The effect of control functions on the reproduction number when $u_1 = 0$.

In the second case, we discuss how intensive prevention and medical care affects the expansion

of COVID-19. For this case, we used $C_1 = 0.7, C_2 = 1.7, B_1 = 225, B_3 = 2220$ and the same initial data and parameter values as above. The corresponding simulation results are illustrated in Fig.4.5. From this figure one can easily see that the number of exposed and infected individuals are highly reduced. That means, at the end of 300 days, approximately the total number of exposed individuals is 8600 while the number of infected individuals nearly 980. Further, it is also important to mention here that the magnitude of $\mathcal{R}_0$ is lower than unity when $u_3 = 0$. Thus, the policy makers may choose intensive prevention such as quarantine, isolation, social distancing and medical care simultaneously in the absence sufficient resource for surface disinfection.

Finally, we present the effects of implementing the three controls strategies: i.e, preventive measures(u_1) including: social distance, tracing patient, quatrain and isolation; intensive medical care (u_1) for all confirmed cases and surface disinfection(u_3) to reduce the concentration of coronavirus from environmental reservoir. In this case we considered the maximum possible value for the three control strategies that minimize the cost functional. The corresponding simulation results are shown in the Fig.4.6. From this figure one can easily conclude that the combination of the three strategies outperform in reducing the disease epidemic and its prevalence. Thus, the best choice is to apply three controls all together to eradicate the epidemic of COVID-19.

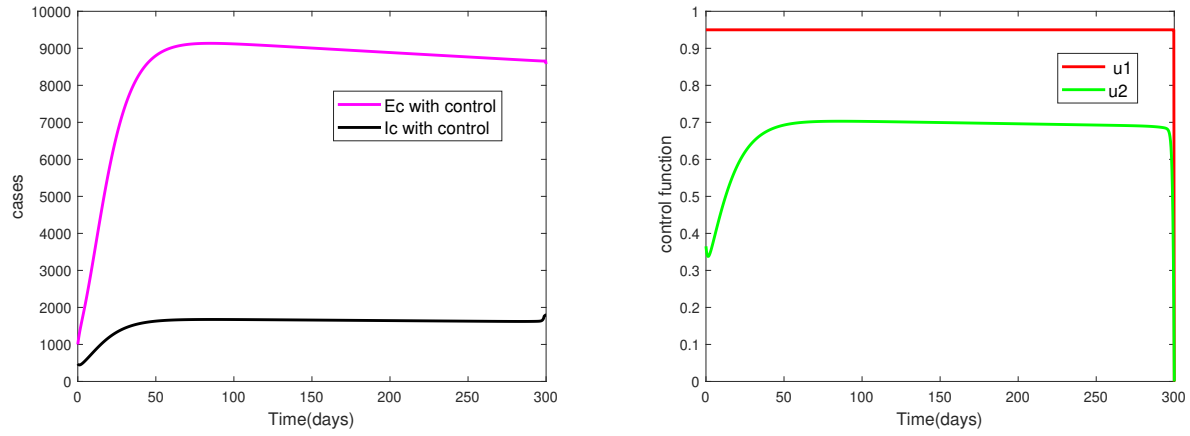

(a) Exposed and infected populations with maxium prevention and optimum medical care.

(b) Profiles of control function when $u_1^{\max}$ and $u_2 \neq 0$.

Figure 4.5: Simulation results for coronavirus outbreak with intensive prevention and medical care.

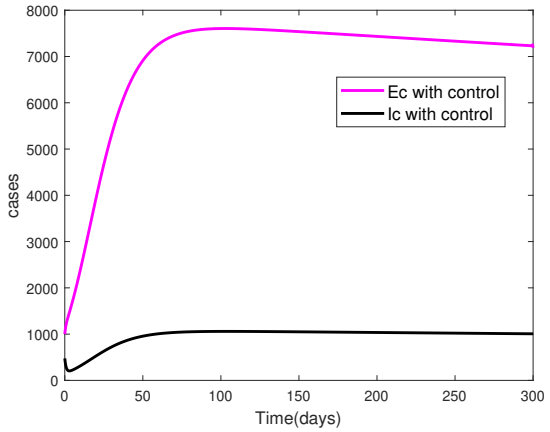

(a) Exposed and infected populations with effective control

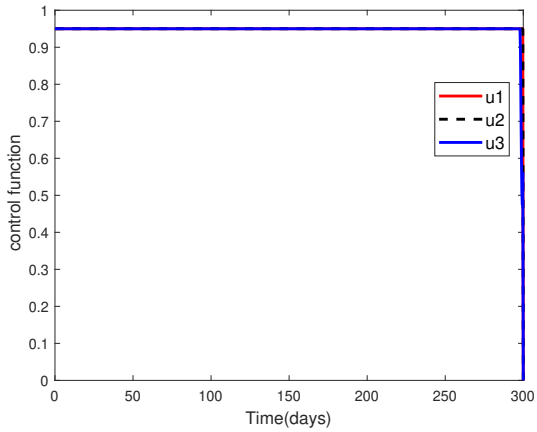

(b) Control profile in the case of $u_1^{\max}$, $u_2^{\max}$ and $u_3^{\max}$.

Figure 4.6: Profiles of exposed and infected population in the case of maximum controls strategy.

CHAPTER 5

MATHEMATICAL MODELING FOR COVID-19 TRANSMISSION DYNAMICS: A CASE STUDY IN ETHIOPIA

5.1 Model Formulation

In this section, we propose an *SEQAIJR* type mathematical model to analyze the dynamics of COVID-19 pandemic. Here, the total population is divided into seven compartments: S denotes susceptible; E represents the compartment of exposed (individuals who may or may not have been infected). We assumed that some of the exposed individuals are quarantined to avoid contact with health individuals. This class is denoted by Q. We assume that asymptomatic individuals contribute to the distribution of the disease and thus denoted by A. A symptomatic individuals who are capable of spreading the disease but not hospitalized are also represented by I. Moreover, seriously sicked and hospitalized individuals are denoted by J. These are isolated individuals with confirmed COVID-19 cases. Lastly, we denote the compartment of recovered individuals by R. Thus, the total population at time t is $N(t) = S(t) + E(t) + Q(t) + A(t) + I(t) + J(t) + R(t)$.

In our model, the parameter Λ denotes the recruitment rate of susceptible individuals. Besides, the population of susceptible are assumed to be increased at the rate ζ due to the influx from quarantined individuals after testing negative. Furthermore, we assumed that the susceptible individuals are acquired infection when they contact either with asymptomatic or symptomatic individuals. In this case, we assumed that the infection rate of asymptomatic individuals is lower than that of symptomatic individuals, with the reduction parameter $\tau \in (0,1)$. This is because of as asymptomatic individuals do not show any symptoms which in turn they do not spread pathogens by sneezing as often as symptomatic individuals. Thus, the force of infection is defined as $\lambda = \dfrac{\beta(\tau A + I)}{N - Q - J}$ excluding the quarantined and isolated from the total population (Bajiya et al., 2020). Here, β denotes the number of new contagions per unit time due to contact with COVID-19 infectious, while $\tau\beta$ stands for the modified transmission coefficient from the susceptible to infected class for asymptomatic class. We represented the natural death rate in each compartment by μ. The term η_1 denotes a fraction of exposed population joining compartment Q, while η_2 represents the portion of individuals moving to compartment A. Furthermore, we denote the proportion of exposed individuals showing symptoms by η_3. The parameter q_1 denotes the rate at which quarantined individual show symptoms and moves to I class. The disease-induced death rates for populations in classes A, I, and J, respectively, are represented by the parameters δ_1, δ_2, and δ_3. The infective individuals in classes A and I are assumed to be recovered at a constant rate r_1 and r_2, respectively, and treated individuals leave compartment J at a rate r_3 joining compartment R. The infected individuals are isolated at a rate α. The resulting mathematical

model is given by a system of nonlinear ordinary differential equations:

$$\begin{cases} \dfrac{dS}{dt} = \Lambda - \lambda S - \mu S + \zeta Q, \\ \dfrac{dE}{dt} = \lambda S - (\eta_1 + \eta_2 + \eta_3 + \mu)E, \\ \dfrac{dQ}{dt} = \eta_1 E - (\zeta + q_1 + \mu)Q, \\ \dfrac{dA}{dt} = \eta_2 E - (r_1 + \delta_1 + \mu)A, \\ \dfrac{dI}{dt} = \eta_3 E + q_1 Q - (\alpha + r_2 + \delta_2 + \mu)I, \\ \dfrac{dJ}{dt} = \alpha I - (r_3 + \delta_3 + \mu)J, \\ \dfrac{dR}{dt} = r_1 A + r_2 I + r_3 J - \mu R, \end{cases} \tag{5.1}$$

where $\lambda = \dfrac{\beta(\tau A + I)}{N - Q - J}$ with initial data $S(0) > 0, E(0) \geq 0, A(0) \geq 0, Q(0) \geq 0, I(0) \geq 0, J(0) \geq 0,$ $R(0) \geq 0$ and $N(0) > 0$. All parameters in the model are assumed to be nonnegative. Compared to the model introduced in (Deressa & Duressa, 2021), our model considers the quarantine of exposed individuals moving either to a susceptible or infected class based on the severity of the disease. Furthermore, COVID-19 induced death rate is also assumed in the asymptomatic individuals. Moreover, compared to the model in (Bajiya et al., 2020), our model considers the asymptomatic compartment. In this case, the asymptomatic individuals move to a recovered class. The descriptions of the model parameters are presented in Table 5.1.

Table 5.1: Model parameters and their definitions.

Parameters	Parameter description
Λ	Recruitment rate
β	Coefficient of transmission
τ	Modification factor for asymptomatic individuals
η_1	The rate at which exposed individuals become quarantined
η_2	Transfer rate of exposed individuals to asymptomatic class
η_3	Rate of exposed individuals showing symptoms after the incubation period
μ	The natural death rate
q_1	The rate at which quarantined individuals become showing symptoms
ζ	Influx from quarantined to susceptible individuals after tested COVID-19 negative
δ_1	Disease related death rate of asymptomatic individuals
δ_2	Disease related death rate of symptomatic individuals
δ_3	Disease related death rate of isolated individuals
α	Rate of infected individuals that are exposed to healthcare treatment
r_1	Recovery rate of asymptomatic individuals
r_2	Recovery rate of infected individuals with symptoms
r_3	Recovery rate of isolated individuals via healthcare treatment

5.2 Model analysis

In this section, some basic properties of the model (5.1) including the existence and uniqueness of the solution, feasible region, the positivity of the solution, equilibria, and their stability are discussed.

Theorem 4 (Existence and uniqueness of solutions)**.** *Solutions to model (5.1) are exists and unique for* $t \in [0,\infty)$.

Proof. The model (5.1) can be written as:

$$\dot{x} = f(t,x(t))$$

where $x(t) = (S(t),E(t),Q(t),A(t),I(t),J(t),R(t))$ and $f(t,x(t)) = (f_1(t,x(t)),\cdots,f_7(t,x(t)))$ denotes the right hand expressions. The result is straightforward: applying the existence and uniqueness theorem in (Hale, 1969), one can easily show that there exists a unique solution for model (5.1) in the bounded region $\mathbb{R}^7_+$. This can be verified by checking that in the bounded region $\mathbb{R}^7_+$, each of the partial derivatives on the right side of the model (5.1) with respect to S, E, Q, A, I, J or R are bounded in $\mathbb{R}^7_+$. □

The next theorem implies that the solutions of the model (5.1) are nonnegative and bounded from above with nonnegative initial conditions.

Theorem 5 (Nonnegativity and boundedness of the solution)**.** *All solutions of model (5.1) with nonnegative initial value remain nonnegative for all $t \geq 0$. Moreover*

$$\lim_{t \longrightarrow \infty} \sup N(t) \leq \frac{\Lambda}{\mu}.$$

Proof. We show that all solutions of the model (5.1) are nonnegative as required in (**??**). We use the proof by contradiction to show that the state variable S of the model is positive for all $t \geq 0$. We suppose that a trajectory crosses the positive cone at time t_1 such that:

- $t_1 : S(t_1) = 0, \frac{dS}{dt}(t_1) < 0, E(t) > 0, Q(t) > 0, A(t) > 0, I(t) > 0, J(t) > 0$, and $R(t) > 0$ for $t \in (0, t_1)$.

Using the first equation of the model (5.1), the first assumption leads to

$$\frac{dS}{dt}(t_1) = \Lambda + \zeta Q(t_1) > 0,$$

which contradicts the first assumption that $\frac{dS}{dt}(t_1) < 0$. Thus, $S(t)$ remains positive for all $t \geq 0$. Here, we choose t_1 in such away that our point to be on the positive axis of $S(t)$ so that $Q(t_1)$ is positive.

Based on the second equation of model (5.1),

$$\frac{dE}{dt} = \lambda S - (\eta_1 + \eta_2 + \eta_3 + \mu)E \geq -(\eta_1 + \eta_2 + \eta_3 + \mu)E,$$

because $S(t)$ is nonnegative for all $t \geq 0$. Solving this equation yields

$$E(t) \geq E(0) \exp\left(-(\eta_1 + \eta_2 + \eta_3 + \mu)t\right) \geq 0.$$

Correspondingly, from the third equation of model (5.1), we obtain

$$\frac{dQ}{dt} = \eta_1 E - (\zeta + q_1 + \mu)Q \geq -(\zeta + q_1 + \mu)Q.$$

Solving this equation leads to

$$Q(t) \geq Q(0) \exp\left(-(\zeta + q_1 + \mu)\right) \geq 0.$$

Similarly, using the last four equations of model (5.1), we have

$$\frac{dA}{dt} = \eta_2 E - (r_1 + \delta_1 + \mu)A \geq -(r_1 + \delta_1 + \mu)A,$$

$$\frac{dI}{dt} = \eta_3 E + q_1 Q - (\alpha + r_2 + \delta_2 + \mu)I \geq -(\alpha + r_2 + \delta_2 + \mu)I,$$

$$\frac{dJ}{dt} = \alpha I - (r_3 + \delta_3 + \mu)J \geq -(r_3 + \delta_3 + \mu)J,$$

and

$$R(t) = r_1 A + r_2 I + r_3 J - \mu R \geq -\mu R,$$

because $S(t)$, $E(t)$, and $Q(t)$ are nonnegative for all $t \geq 0$. Solving the above equations gives

$$A(t) \geq A(0)\exp\left(-(r_1 + \delta_1 + \mu)t\right) \geq 0,$$

$$I(t) \geq I(0)\exp\left(-(\alpha + r_2 + \delta_2 + \mu)t\right) \geq 0,$$

$$J(t) \geq J(0)\exp\left(-(r_3 + \delta_3 + \mu)t\right) \geq 0,$$

and

$$R(t) \geq R(0)\exp(-\mu t) \geq 0.$$

respectively. Thus, any solution of model (5.1) is nonnegative with nonnegative initial data for all $t \geq 0$. Furthermore, adding the right-hand sides of model (5.1) together, we obtain

$$\frac{dN}{dt} = \Lambda - \mu N - (\delta_1 A + \delta_2 I + \delta_3 J) \ \leq \Lambda - \mu N.$$

It follows that

$$N(t) \leq \frac{\Lambda}{\mu} + \left(N(0) - \frac{\Lambda}{\mu}\right) e^{-\mu t}.$$

Considering $t \longrightarrow \infty$, we have

$$\lim_{t \longrightarrow \infty} \sup N(t) \leq \frac{\Lambda}{\mu}.$$

Thus, the model (5.1) is bounded. This completes the proof of Theorem 5. □

Theorem 6. *The closed region*

$$\Omega = \left\{(S, E, Q, A, I, J, R) \in \mathbb{R}^7_+ : 0 < S + E + Q + A + I + J + R \leq \frac{\Lambda}{\mu}\right\}$$

is positively invariant set for the model (5.1).

Proof. Positive invariance of $\mathbb{R}^7_+$ can be verified by examining the direction of the vector field $(f_1, f_2, f_3, f_4, f_5, f_6, f_7)^T$ of the model (5.1) on each face (**?**). Thus, to show that $\mathbb{R}^7_+$ is positively invariant, it suffices to show that the direction of the vector field points inward on the boundary of $\mathbb{R}^7_+$.

For example, for the model (5.1), on the face $S = 0$, we have

$$\frac{dS}{dt}|_{S=0} = \Lambda + \zeta Q \ > 0.$$

Therefore, the vector field on the (E,Q,A,I,J,R)-face points to the interior of $\mathbb{R}^7_+$. No solution can escape the interior through the (E,Q,A,I,J,R)-face. Similarly, one can show for the others. If $N = S+E+Q+A+I+J+R = \dfrac{\Lambda}{\mu}$,

$$\frac{dN}{dt}|_{N=\frac{\Lambda}{\mu}} = -(\delta_1 A + \delta_2 I + \delta_3 J) \leq 0.$$

We thus have shown that all solutions starting in $\mathbb{R}^7_+$ remain in $\mathbb{R}^7_+$ for $t > 0$. That is, Ω is positively invariant for the model (5.1). □

5.2.1 Disease free equilibrium

We calculate the disease-free equilibrium of model (5.1) by equating the right-hand side equations to zero and then putting $E = 0, Q = 0, A = 0, I = 0$, and $J = 0$. Then we get;

$$E^0 = (S^0,0,0,0,0,0,0) = \left(\frac{\Lambda}{\mu},0,0,0,0,0,0\right).$$

The infected compartments of model (5.1) consist of (E,Q,A,I,J) classes. Using the next generation method (Diekmann et al., 2010; Van den Driessche & Watmough, 2002), the basic reproduction number R_0 can be calculated from the relation $R_0 = \rho(FV^{-1})$ (the spectral radius of the Eigenvalue of the Jacobian matrix evaluated at the COVID-19-free equilibrium point E^0). The Jacobian matrix calculated at E^0 of the transmission terms, F and that of transition terms, V are, respectively

$$F = \begin{pmatrix} 0 & 0 & \beta\tau & \beta & 0 \\ 0 & 0 & 0 & 0 & 0 \\ 0 & 0 & 0 & 0 & 0 \\ 0 & 0 & 0 & 0 & 0 \\ 0 & 0 & 0 & 0 & 0 \end{pmatrix}$$

and

$$V = \begin{pmatrix} K_1 & 0 & 0 & 0 & 0 \\ -\eta_1 & K_2 & 0 & 0 & 0 \\ -\eta_2 & 0 & K_3 & 0 & 0 \\ -\eta_3 & -q_1 & 0 & K_4 & 0 \\ 0 & 0 & 0 & -\alpha & K_5 \end{pmatrix},$$

where $K_1 = \eta_1 + \eta_2 + \eta_3 + \mu$, $K_2 = \zeta + q_1 + \mu$, $K_3 = r_1 + \delta_1 + \mu$, $K_4 = \alpha + r_2 + \delta_2 + \mu$ and $K_5 = r_3 + \delta_3 + \mu$. Thus, the next generation matrix is

$$FV^{-1} = \begin{pmatrix} \frac{\beta\tau\eta_2}{K_1K_3} + \frac{\beta(\eta_3K_2 + \eta_1q_1)}{K_1K_2K_4} & \frac{\beta q_1}{K_2K_4} & \frac{\beta\tau}{K_3} & \frac{\beta}{K_4} & 0 \\ 0 & 0 & 0 & 0 & 0 \\ 0 & 0 & 0 & 0 & 0 \\ 0 & 0 & 0 & 0 & 0 \\ 0 & 0 & 0 & 0 & 0 \end{pmatrix}.$$

By solving the dominant eigenvalue of the next generation matrix FV^{-1}, we get the basic reproduction number

$$\begin{aligned} R_0 &= \frac{\beta[\tau\eta_2K_2K_4 + K_3(\eta_3K_2 + \eta_1q_1)]}{K_1K_2K_3K_4} \\ &= \frac{\beta[\tau\eta_2(\zeta + q_1 + \mu)(\alpha + r_2 + \delta_2 + \mu) + (r_1 + \delta_1 + \mu)(\eta_3(\zeta + q_1 + \mu) + \eta_1q_1)]}{(\eta_1 + \eta_2 + \eta_3 + \mu)(\zeta + q_1 + \mu)(r_1 + \delta_1 + \mu)(\alpha + r_2 + \delta_2 + \mu)}. \end{aligned}$$

Remark 2. *The basic reproduction number, R_0 is defined as the expected number of secondary infections produced by an index case in a completely susceptible population by a typical infective individual (Diekmann et al., 2010). This number is a measure of the potential for disease spread within a population. Mathematically, R_0 is a threshold for the stability of a disease-free equilibrium and that can be used as an indicator for disease control.*

5.2.2 Local and global stability of DFE

In many epidemiological models, there is a disease-free equilibrium point (DFE) at which the population remains in the absence of disease. The following theorems discuss the local and global stability of DFE E^0.

Theorem 7. *The disease-free equilibrium E^0 of model (5.1) is locally asymptotically stable if $R_0 < 1$ and unstable if $R_0 > 1$.*

Proof. We determine the local stability of DFE (E^0) using the eigenvalues of the Jacobian matrix at E^0, which is given by

$$J_{E^0} = \begin{pmatrix} -\mu & 0 & \zeta & -\beta\tau & -\beta & 0 & 0 \\ 0 & -K_1 & 0 & \beta\tau & \beta & 0 & 0 \\ 0 & \eta_1 & -K_2 & 0 & 0 & 0 & 0 \\ 0 & \eta_2 & 0 & -K_3 & 0 & 0 & 0 \\ 0 & \eta_3 & q_1 & 0 & -K_4 & 0 & 0 \\ 0 & 0 & 0 & 0 & \alpha & -K_5 & 0 \\ 0 & 0 & 0 & r_1 & r_2 & r_3 & -\mu \end{pmatrix}.$$

where $K_1 = \eta_1 + \eta_2 + \eta_3 + \mu$, $K_2 = \zeta + q_1 + \mu$, $K_3 = r_1 + \delta_1 + \mu$, $K_4 = \alpha + r_2 + \delta_2 + \mu$ and $K_5 = r_3 + \delta_3 + \mu$ as in section (5.2.1). It is obvious that $\lambda_1 = -\mu$, $\lambda_6 = -K_5$ and $\lambda_7 = -\mu$ are three negative eigenvalues of J_{E^0}. We find the remaining eigenvalues of J_{E^0} from the following block matrix

$$RJ_{E^0} = \begin{pmatrix} -K_1 & 0 & \beta\tau & \beta \\ \eta_1 & -K_2 & 0 & 0 \\ \eta_2 & 0 & -K_3 & 0 \\ \eta_3 & q_1 & 0 & -K_4 \end{pmatrix}.$$

The characteristic polynomial of RJ_{E^0} is given by

$$P(\lambda) = \lambda^4 + a_1\lambda^3 + a_2\lambda^2 + a_3\lambda + a_4,$$

where

$$a_1 = K_1 + K_2 + K_3 + K_4,$$

$$a_2 = K_1(K_2 + K_3 + K_4) + K_2(K_3 + K_4) + K_3K_4 - \beta(\eta_3 + \tau\eta_2),$$

$$a_3 = K_1K_2(K_3 + K_4) + K_3K_4(K_1 + K_2) - \beta[\eta_3(K_2 + K_3) + \tau\eta_2(K_2 + K_4) + \eta_1q_1],$$

$$a_4 = K_1K_2K_3K_4(1 - R_0).$$

Applying the Routh-Hurwitz stability criterion (Allen, 2007) and after some little algebraic manipulations, it can be shown that the eigenvalues of the block matrix RJ_{E^0} have negative real parts i.e. $\Re(\lambda_2), \Re(\lambda_3), \Re(\lambda_4), \Re(\lambda_5) < 0$, if $R_0 < 1$. If $R_0 > 1$, then $a_3 < 0$, thus the matrix RJ_{E^0} has at least one eigenvalue with positive real part. Hence, disease-free equilibrium (E^0) of model (5.1) is locally asymptotically stable if $R_0 < 1$ and unstable if $R_0 > 1$. □

From the above theorem, we conclude that if $R_0 < 1$, then the DFE is locally asymptotically stable, and the disease cannot invade the population; but if $R_0 > 1$, then the DFE is unstable and invasion is always possible. In the next theorem, the global stability of disease-free equilibrium is investigated by using the technique implemented in (Castillo-Chavez & Song, 2004).

Theorem 8. *If $R_0 < 1$, the disease-free equilibrium E^0 of model (5.1) is globally asymptotically stable in its feasible region.*

Proof. First, we rewrite the model (5.1) as follows:

$$\frac{dX}{dt} = F(X,Y),$$

$$\frac{dY}{dt} = G(X,Y), \text{ with } G(X,0) = 0,$$

where $X = (S,R) \in \mathbb{R}^2$ represents the non-disease compartments, and $Y = (E,Q,A,I,J) \in \mathbb{R}^5$ represents the disease compartments. The following two conditions (H_1) and (H_2) are required for the global asymptotic stability of the DFE of model (5.1).

(H_1) For $\dfrac{dX}{dt} = F(X,0)$, X^* is globally asymptotically stable, where $F(X^*,0) = 0$.

(H_2) $G(X,Y) = BY - \tilde{G}(X,Y)$, $\tilde{G}(X,Y) > 0$ for $(X,Y) \in \Omega$, where $B = D_Y G(X^*,0)$ is an M-matrix. The off-diagonal elements of B are nonnegative and is the region where the system makes biologically feasible in Ω.

For model (5.1), we have

$$\frac{dX}{dt} = \begin{pmatrix} \Lambda - \mu S \\ 0 \end{pmatrix}. \tag{5.2}$$

Indeed, the system (5.2) is globally asymptotically stable around $X^* = \left(\dfrac{\Lambda}{\mu}, 0\right)$. This can be verified from the solution $S(t) = \dfrac{\Lambda}{\mu} + (S(0) - \dfrac{\Lambda}{\mu})e^{-\mu t}$ such that $\lim\limits_{t \longrightarrow \infty} S(t) = \dfrac{\Lambda}{\mu}$, which implies that the global convergence of (5.2) in Ω. Furthermore, from the model (5.1), we obtain

$$B = \begin{pmatrix} -K_1 & 0 & \beta\tau & \beta & 0 \\ \eta_1 & -K_2 & 0 & 0 & 0 \\ \eta_2 & 0 & -K_3 & 0 & 0 \\ \eta_3 & q_1 & 0 & -K_4 & 0 \\ 0 & 0 & 0 & \alpha & -K_5 \end{pmatrix}$$

and

$$\tilde{G}(X,Y) = \begin{pmatrix} \beta(\tau A + I)\left(\dfrac{E+A+I+R}{S+E+A+I+R}\right) \\ 0 \\ 0 \\ 0 \\ 0 \end{pmatrix}$$

Clearly, $\left(\dfrac{E+A+I+R}{S+E+A+I+R}\right) \geq 0$ inside Ω and therefore, $\tilde{G}(X,Y) \geq 0$. Thus, the two conditions (H_1) and (H_2) are satisfied. Therefore, the DFE E^0 of model (5.1) is globally asymptotically stable when $R_0 < 1$. □

5.2.3 Existence of an endemic equilibrium

In this subsection, we investigate the existence of the endemic equilibrium E_1^* of model (5.1).

Theorem 9. *If $R_0 > 1$, there exists a unique endemic equilibrium $E_1^* = (S^*,E^*,Q^*,A^*,I^*,J^*,R^*)$ of system (5.1) and there is no endemic equilibrium when $R_0 < 1$.*

Proof. For the existence of an endemic equilibrium, we need to solve the following system of equations:

$$\begin{cases} \Lambda - \dfrac{\beta S^*(\tau A^* + I^*)}{N - Q^* - J^*} - \mu S^* + \zeta Q^* = 0, \\ \dfrac{\beta S^*(\tau A^* + I^*)}{N - Q^* - J^*} - (\eta_1 + \eta_2 + \eta_3 + \mu)E^* = 0, \\ \eta_1 E^* - (\zeta + q_1 + \mu)Q^* = 0, \\ \eta_2 E^* - (r_1 + \delta_1 + \mu)A^* = 0, \\ \eta_3 E^* + q_1 Q^* - (\alpha + r_2 + \delta_2 + \mu)I^* = 0, \\ \alpha I^* - (r_3 + \delta_3 + \mu)J^* = 0, \\ r_1 A^* + r_2 I^* + r_3 J^* - \mu R^* = 0. \end{cases} \tag{5.3}$$

We use the same definition as in section (5.2.2), $K_1 = \eta_1 + \eta_2 + \eta_3 + \mu$, $K_2 = \zeta + q_1 + \mu$, $K_3 = r_1 + \delta_1 + \mu$, $K_4 = \alpha + r_2 + \delta_2 + \mu$ and $K_5 = r_3 + \delta_3 + \mu$. Solving the above system of equations (5.3) yields

$$S^* = \frac{\Lambda[K_2K_4K_5(\mu K_3 + \eta_2\mu + \eta_2 r_1) + K_3(\mu K_5 + r_2K_5 + r_3\alpha)(\eta_3K_2 + \eta_1 q_1)]}{\mu[K_3K_4K_5(K_1K_2 - \zeta\eta_1)(R_0 - 1) + K_2K_4K_5(\mu K_3 + \eta_2\mu + \eta_2 r_1) + K_3(\mu K_5 + r_2K_5 + r_3\alpha)(\eta_3K_2 + \eta_1 q_1)]},$$

$$Q^* = \frac{\eta_1}{K_2}E^*, \quad A^* = \frac{\eta_2}{K_3}E^*, \quad I^* = \frac{\eta_3K_2 + \eta_1 q_1}{K_2K_4}E^*,$$

$$J^* = \frac{\alpha(\eta_3K_2 + \eta_1 q_1)}{K_2K_4K_5}E^*, \quad R^* = \frac{r_1\eta_2K_2K_4K_5 + K_3(r_2K_5 + r_3\alpha)(\eta_3K_2 + \eta_1 q_1)}{K_2K_3K_4K_5\mu}E^*,$$

$$E^* = \frac{K_2K_3K_4K_5\mu(R_0 - 1)S^*}{K_2K_4K_5(\mu K_3 + \eta_2\mu + \eta_2 r_1) + K_3(\mu K_5 + r_2K_5 + r_3\alpha)(\eta_3K_2 + \eta_1 q_1)}.$$

Since $K_1K_2 - \zeta\eta_1 = \eta_1(q_1 + \mu) + (\eta_2 + \eta_3 + \mu)(\zeta + q_1 + \mu) > 0$, we can easily observe that there exists a unique endemic equilibrium of the model (5.1) when $R_0 > 1$ and no endemic equilibrium when $R_0 < 1$. □

5.2.4 Bifurcation analysis

In this subsection, we establish the conditions on the parameters using Theorem 4.1 from (Castillo-Chavez & Song, 2004) and center manifold theory (Guckenheimer & Holmes, 2013). In this theorem, there are two coefficients that represent dynamics on the centre manifold. If we say these coefficients that 'decide' the bifurcation a and b, we have $a < 0$ and $b > 0$ for the occurrence of forward bifurcation.

First, we choose the transmission rate β as a bifurcation parameter. By solving $R_0 = 1$, we obtain

$$\beta = \beta^* = \frac{(\eta_1 + \eta_2 + \eta_3 + \mu)(\zeta + q_1 + \mu)(r_1 + \delta_1 + \mu)(\alpha + r_2 + \delta_2 + \mu)}{\tau\eta_2(\zeta + q_1 + \mu)(\alpha + r_2 + \delta_2 + \mu) + (r_1 + \delta_1 + \mu)(\eta_3(\zeta + q_1 + \mu) + \eta_1 q_1)}.$$

The Jacobian matrix $J_{(E^0,\beta^*)}$ for the model (5.1) evaluated at E^0 and $\beta = \beta^*$ has a simple zero eigenvalue and other eigenvalues have negative sign. Hence E^0 is a non-hyperbolic equilibrium, when $\beta = \beta^*$. Therefore, we can use the center manifold theory (Castillo-Chavez & Song, 2004; Guckenheimer & Holmes, 2013) to establish the local stability of the endemic equilibrium E^*. Calculating a right eigenvector $W = (w_1, w_2, w_3, w_4, w_5, w_6, w_7)^T$ and a left eigenvector $V = (v_1, v_2, v_3, v_4, v_5, v_6, v_7)$ associated to the zero eigenvalues, we get

$$w_1 = -\frac{K_3K_4K_5(K_1K_2 - \zeta\eta_1)}{r_1\eta_2K_2K_4K_5 + K_3(r_2K_5 + r_3\alpha)(\eta_3K_2 + \eta_1q_1)},$$

$$w_2 = \frac{\mu K_2K_3K_4K_5}{r_1\eta_2K_2K_4K_5 + K_3(r_2K_5 + r_3\alpha)(\eta_3K_2 + \eta_1q_1)},$$

$$w_3 = \frac{\mu\eta_1K_3K_4K_5}{r_1\eta_2K_2K_4K_5 + K_3(r_2K_5 + r_3\alpha)(\eta_3K_2 + \eta_1q_1)},$$

$$w_4 = \frac{\mu\eta_2K_2K_4K_5}{r_1\eta_2K_2K_4K_5 + K_3(r_2K_5 + r_3\alpha)(\eta_3K_2 + \eta_1q_1)},$$

$$w_5 = \frac{\mu K_3K_5(\eta_3K_2 + \eta_1q_1)}{r_1\eta_2K_2K_4K_5 + K_3(r_2K_5 + r_3\alpha)(\eta_3K_2 + \eta_1q_1)}$$

$$w_6 = \frac{\alpha\mu K_3(\eta_3K_2 + \eta_1q_1)}{r_1\eta_2K_2K_4K_5 + K_3(r_2K_5 + r_3\alpha)(\eta_3K_2 + \eta_1q_1)}, \quad w_7 = 1$$

and

$$v_1 = 0, \quad v_2 = \frac{\tau\eta_2K_2K_4 + K_3(\eta_3K_2 + \eta_1q_1)}{K_1K_2K_3}, \quad v_3 = \frac{q_1}{K_2}, \quad v_4 = \frac{\tau K_4}{K_3},$$

$$v_5 = 1, \quad v_6 = 0, \quad v_7 = 0.$$

Now from Theorem 4.1 of (Castillo-Chavez & Song, 2004), we need to calculate the bifurcation constants a and b :

$$a = \sum_{k,i,j=1}^{7} v_k w_i w_j \frac{\partial^2 f_k}{\partial x_i \partial x_j}(E^0, \beta^*)$$

$$b = \sum_{k,i=1}^{7} v_k w_i \frac{\partial^2 f_k}{\partial x_i \partial \beta}(E^0, \beta^*).$$

Denote $x_1 = S$, $x_2 = E$, $x_3 = Q$, $x_4 = A$, $x_5 = I$, $x_6 = J$, $x_7 = R$. Since $v_1 = 0$, $v_6 = 0$ and $v_7 = 0$, we don't need the derivatives of f_1, f_6 and f_7. From the second-order partial derivatives of f_2, f_3, f_4 and f_5, the only ones that are nonzero are the following:

$$\frac{\partial^2 f_2}{\partial x_4 \partial x_2}(E^0, \beta^*) = \frac{\partial^2 f_2}{\partial x_2 \partial x_4}(E^0, \beta^*) = -\frac{\beta^*\tau\mu}{\Lambda}, \quad \frac{\partial^2 f_2}{\partial x_4 \partial x_4}(E^0, \beta^*) = -\frac{2\beta^*\tau\mu}{\Lambda},$$

$$\frac{\partial^2 f_2}{\partial x_5 \partial x_2}(E^0, \beta^*) = \frac{\partial^2 f_2}{\partial x_2 \partial x_5}(E^0, \beta^*) = -\frac{\beta^*\mu}{\Lambda}, \quad \frac{\partial^2 f_2}{\partial x_5 \partial x_4}(E^0, \beta^*) = \frac{\partial^2 f_2}{\partial x_4 \partial x_5}(E^0, \beta^*) = -\frac{\beta^*(1+\tau)\mu}{\Lambda},$$

$$\frac{\partial^2 f_2}{\partial x_7 \partial x_4}(E^0,\beta^*) = \frac{\partial^2 f_2}{\partial x_4 \partial x_7}(E^0,\beta^*) = -\frac{\beta^*\tau\mu}{\Lambda}, \quad \frac{\partial^2 f_2}{\partial x_5 \partial x_5}(E^0,\beta^*) = -\frac{2\beta^*\mu}{\Lambda},$$

$$\frac{\partial^2 f_2}{\partial x_7 \partial x_5}(E^0,\beta^*) = \frac{\partial^2 f_2}{\partial x_5 \partial x_7}(E^0,\beta^*) = -\frac{\beta^*\mu}{\Lambda}.$$

Furthermore,

$$\frac{\partial^2 f_2}{\partial x_4 \partial \beta}(E^0,\beta^*) = \tau, \quad \frac{\partial^2 f_2}{\partial x_5 \partial \beta}(E^0,\beta^*) = 1.$$

Hence, we obtain

$$\begin{aligned}
a &= v_2\left[2\left(w_4w_2\frac{\partial^2 f_2}{\partial A\partial E} + w_5w_2\frac{\partial^2 f_2}{\partial I\partial E} + w_5w_4\frac{\partial^2 f_2}{\partial I\partial A} + w_7w_4\frac{\partial^2 f_2}{\partial R\partial A} + w_7w_5\frac{\partial^2 f_2}{\partial R\partial I}\right) + w_4^2\frac{\partial^2 f_2}{\partial A^2} + w_5^2\frac{\partial^2 f_2}{\partial I^2}\right] \\
&= -v_2\frac{\beta^*\mu}{\Lambda}\left[2\left(w_4w_2\tau + w_5w_2 + w_5w_4(1+\tau) + w_7w_4\tau + w_7w_5\right) + 2(w_4^2\tau + w_5^2)\right] \\
&= -2v_2\frac{\beta^*\mu}{\Lambda}\left[w_4w_2\tau + w_5w_2 + w_5w_4(1+\tau) + w_7w_4\tau + w_7w_5 + w_4^2\tau + w_5^2\right] < 0, \\
b &= v_2\left(w_4\frac{\partial^2 f_2}{\partial A\partial\beta} + w_5\frac{\partial^2 f_2}{\partial I\partial\beta}\right) \\
&= v_2(w_4\tau + w_5) > 0.
\end{aligned}$$

Clearly, $a < 0$ and $b > 0$, at $\beta = \beta^*$. Therefore, by applying Theorem 4.1 stated in (Castillo-Chavez & Song, 2004), the model (5.1) undergoes a forward/transcritical bifurcation at $R_0 = 1$ (See the Fig. 5.10). Hence, we get the following result.

Lemma 10. *(Local stability of endemic equilibrium). The unique endemic equilibrium E^* of model (5.1) is locally asymptotically stable (LAS) if $R_0 > 1$.*

The forward bifurcation tell us that as the basic reproduction number crosses a critical value, $R_0 = 1$ the system transit from one equilibrium point, which is typically stable, to two non-negative equilibrium points, with one stable and one unstable. This implies that COVID-19 disease cannot invade the population for $R_0 < 1$. On the contrary, the disease persist in the community for R_0 exceeds unity.

5.2.5 Global stability analysis of endemic equilibrium point

Here, we apply the high-dimensional Bendixson criterion which is developed in (Y. Li & Muldowney, 1993) to prove the global stability of the endemic equilibrium point E_1^*. The following lemma will be useful in the sequel before proving the global stability of the endemic equilibrium point E_1^*.

Lemma 11. *The model (5.1) has no periodic orbits.*

Proof. We establish the Dulac's criterion to prove the theorem. Let $X = (S,E,Q,A,I,J,R)$. Define

the Dulac's function

$$B = \frac{1}{SQ}.$$

Then we obtain

$$\begin{aligned}
\frac{dBX}{dt} &= \frac{\partial}{\partial S}\left(B\frac{dS}{dt}\right) + \frac{\partial}{\partial E}\left(B\frac{dE}{dt}\right) + \frac{\partial}{\partial Q}\left(B\frac{dQ}{dt}\right) + \frac{\partial}{\partial A}\left(B\frac{dA}{dt}\right) + \frac{\partial}{\partial I}\left(B\frac{dI}{dt}\right) \\
&+ \frac{\partial}{\partial J}\left(B\frac{dJ}{dt}\right) + \frac{\partial}{\partial R}\left(B\frac{dR}{dt}\right) \\
&= \frac{\partial}{\partial S}\left(\frac{\Lambda}{SQ} - \frac{\beta(\tau A + I)}{Q(N-Q-J)} - \frac{\mu}{Q} + \frac{\zeta}{S}\right) + \frac{\partial}{\partial E}\left(\frac{\beta(\tau A + I)}{Q(N-Q-J)} - \frac{K_1 E}{SQ}\right) \\
&+ \frac{\partial}{\partial Q}\left(\frac{\eta_1 E}{SQ} - \frac{K_2}{S}\right) + \frac{\partial}{\partial A}\left(\frac{\eta_2 E}{SQ} - \frac{K_3 A}{SQ}\right) + \frac{\partial}{\partial I}\left(\frac{\eta_3 E}{SQ} + \frac{q_1}{S} - \frac{K_4 I}{SQ}\right) \\
&+ \frac{\partial}{\partial J}\left(\frac{\alpha I}{SQ} - \frac{K_5 J}{SQ}\right) + \frac{\partial}{\partial R}\left(\frac{r_1 A}{SQ} + \frac{r_2 I}{SQ} + \frac{r_3 J}{SQ} - \frac{\mu R}{SQ}\right) \\
&= -\left[\frac{\Lambda}{QS^2} + \frac{\zeta}{S^2} + \frac{\eta_1 E}{SQ^2} + \frac{K_1 + K_3 + K_4 + K_5 + \mu}{SQ}\right] \\
&< 0.
\end{aligned}$$

Hence, Dulac's criterion implies that there does not exist any periodic solution in Ω for the model (5.1). □

From an epidemiological point of view, the non-existence of periodic orbit implies that there are fluctuations in the number of infectives which makes it difficult to allocate resources for disease control.

Theorem 12. *The endemic equilibrium E_1^* of model (5.1) is globally asymptotically stable whenever $R_0 > 1$.*

Proof. The result can be established by using the approach given in (I. Ahmed et al., 2021; Y. Li & Muldowney, 1993) and Lemma 11. □

5.3 Parameter estimation

In this section, we estimate the parameters in model (5.1) based on real data of COVID-19 infected cases in Ethiopia. In this study, we consider the COVID-19 monthly confirmed cases from March 13, 2020, until July 31, 2021 in Ethiopia (see Table 5.2). The data were collected from Ethiopian Public Health Institute (EPHI) which is also available online at (by the Center for Systems Science & at Johns Hopkins University (JHU, 2021). The COVID-19 data for Ethiopia are fitted using the nonlinear least-squares curve fitting method with the help of "*fminsearch*" function from the MATLAB Optimization Toolbox. Some of the model parameters are estimated from the literature. The average life expectancy of Ethiopians for the year 2021 is 67.8 (Deressa

& Duressa, 2021) and hence, the natural death rate of individuals is calculated by taking the reciprocal of the average life expectancy (in months) which is $\mu = 1/(67.8 \times 12)$. The total population of Ethiopia for the year 2021 is estimated about $N(0) = 114,963,588$ people (Deressa & Duressa, 2021). The recruitment rate of susceptible individuals (Λ) is obtained from $\Lambda/\mu = N(0)$, and it is assumed to be $141,302$. The incubation period ($1/\eta_3$) for COVID-19, which is the time from exposure to symptom development, is on average five to seven days. The quarantine period ($1/\zeta$) for COVID-19 is 2 weeks.

To estimate the rest of parameters, the initial conditions for the state variables are used. According to EPHI report, in March 2020, there have been 26 COVID-19 confirmed cases in Ethiopia, so that $I(0) = 26$. As in other parts of the world, also in Ethiopia there is a limited COVID-19 test and there is the possibility for the presence of asymptomatic individuals (infected individuals with no symptoms) (Deressa & Duressa, 2021). This results the actual number of cases is more likely higher than the reported cases. Thus, we estimate the initial conditions for the exposed, asymptomatic, quarantined, isolated, and recovered individuals to account for the possible actual number of cases. Now, it is easy to determine the initial susceptible population as $S(0) = N(0) - (E(0) + Q(0) + A(0) + I(0) + J(0) + R(0))$. Therefore, we can assume the initial conditions for the state variables used in model fitting to the real data as follows: $E(0) = 5000$, $Q(0) = 6000$, $A(0) = 600$, $J(0) = 24$ and $R(0) = 500$.

The best fit to the monthly reported active cases via our model is displayed in Fig. 5.1. The values of the calculated and estimated parameters are summarized in Table 5.3 and it is to be noted that the values of the parameters used in this work are obtained from estimation, model fitting and from the literature and the unit of parameters (rate constants) is per month. Using the parameter values in Table 5.3, the basic reproductive value is $R_0 = 1.0029$, which is greater than COVID-19 threshold value 1.

Table 5.2: COVID-19 total confirmed cases in Ethiopia (by the Center for Systems Science & at Johns Hopkins University (JHU, 2021).

Months	Total confirmed cases	Months	Total confirmed cases
March 31, 2020	26	Dec 31, 2020	124264
April 30, 2020	131	Jan 31, 2021	137650
May 31, 2020	1172	Feb 28, 2021	159072
June 30, 2020	5846	March 31, 2021	206589
July 31, 2020	17530	Apr 30, 2021	257442
August 31, 2020	52131	May 31, 2021	271541
Sep 30, 2020	75368	June 30, 2021	276174
Oct 31, 2020	96169	July 31, 2021	280365
Nov 30, 2020	110074		

Table 5.3: Parameter values

Parameters	Values	Reference
Λ	141302	Calculated using Deressa & Duressa (2021)
μ	0.001229	Deressa & Duressa (2021)
η_3	$1/7$	Bugalia et al. (2020)
ζ	$1/14$	Bugalia et al. (2020)
β	0.88	Fitted
α	0.75214	Fitted
r_1	0.00827	Fitted
r_2	0.00787	Fitted
r_3	0.20186	Fitted
δ_1	0.16673	Fitted
δ_2	0.00147	Fitted
δ_3	0.00038	Fitted
q_1	0.31167	Fitted
η_1	0.81692	Fitted
η_2	0.02557	Fitted
τ	0.45	Fitted

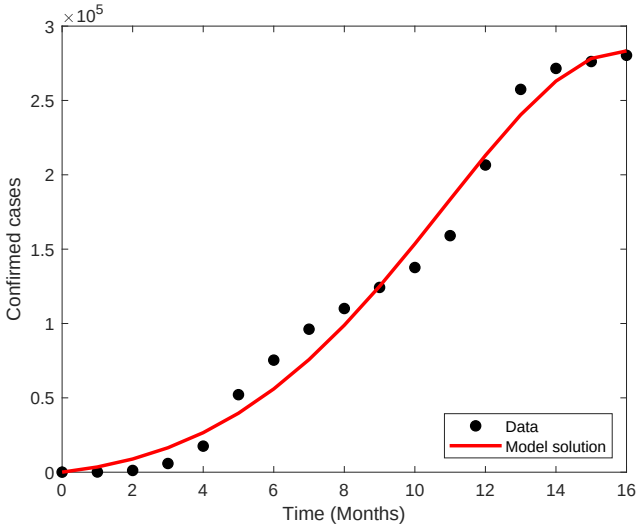

Figure 5.1: The fitted data to the reported cases using model (5.1) for Ethiopia from March 13, 2020 to July 31, 2021.

5.4 Sensitivity analysis

In this section, the sensitivity of model parameters with respect to the basic reproduction number R_0 is performed and analyzed to limit COVID-19 cases for Ethiopia. To implement the sensitivity analysis, we calculate the sensitivity indices of the reproductive number,R_0, to the parameters in the model. To investigate the most influential control parameters, we compute the normalized forward sensitivity indices, which tell us how crucial each parameter is to disease transmission and prevalence. Mathematically, using the approach in (Chitnis et al., 2008), we can define the normalized forward sensitivity index of a variable, M, which depends differentiably on a parameter, p, as

$$\Upsilon_p^M = \frac{\partial M}{\partial p} \times \frac{p}{M}.$$

From an explicit formula for R_0,

$$R_0 = \frac{\beta[\tau\eta_2(\zeta+q_1+\mu)(\alpha+r_2+\delta_2+\mu)+(r_1+\delta_1+\mu)(\eta_3(\zeta+q_1+\mu)+\eta_1 q_1)]}{(\eta_1+\eta_2+\eta_3+\mu)(\zeta+q_1+\mu)(r_1+\delta_1+\mu)(\alpha+r_2+\delta_2+\mu)},$$

we derive an analytical expression for the normalized forward sensitivity indices of R_0 to different parameters involved in R_0. For example,

$$\Upsilon_\beta^{R_0} = \frac{\partial R_0}{\partial \beta} \times \frac{\beta}{R_0} = 1.$$

is the normalized forward sensitivity indices of R_0 with respect to the parameter β. Similarly, we can find for the remaining parameters. The sensitivity indices evaluated at the baseline parameter values are given in Table 5.3 were written in Table 5.4.

Table 5.4: The normalized forward sensitivity indices of R_0 to model parameters evaluated at the baseline parameter values listed in Table 5.3.

Parameters	Sensitivity indices	Values
β	$\Upsilon_{\beta}^{R_0}$	$+1$
q_1	$\Upsilon_{q_1}^{R_0}$	$+0.146459$
τ	$\Upsilon_{\tau}^{R_0}$	$+0.058236$
η_2	$\Upsilon_{\eta_2}^{R_0}$	$+0.032318$
η_3	$\Upsilon_{\eta_3}^{R_0}$	$+0.022257$
α	$\Upsilon_{\alpha}^{R_0}$	-0.928714
ζ	$\Upsilon_{\zeta}^{R_0}$	-0.143982
η_1	$\Upsilon_{\eta_1}^{R_0}$	-0.053329
r_1	$\Upsilon_{r_1}^{R_0}$	-0.002733
r_2	$\Upsilon_{r_2}^{R_0}$	-0.009718

From Table 5.4, parameters with positive sensitivity indices implies that an increase in that parameter's values will have a major effect on the frequency of the disease spread. For example, from $\Upsilon_{\beta}^{R_0} = 1$, we can see that increasing (or decreasing) the contact rate β by 10%, increase (or decrease) the R_0 by 10%. On the other hand, parameters with negative sensitivity indices implies that an increase in the importance of these parameters would help to decrease the violence of the disease. For example, the increasing (or decreasing) rate of exposed individuals become quarantined η_1 by 10%, decrease (or increase) the R_0 by 10%.

In addition, the contour plots of the basic reproduction number R_0 irrespective of different parameters of the model (5.1) are illustrated in Figs. 5.2–5.6 to investigate the effect of the control parameters on R_0. In Fig. 5.2, the contours shows that increasing the individuals joining the susceptible group from quarantine after the negative test of COVID-19 reduces the amount of basic reproduction number and, therefore, COVID cases, while the increase of coefficient of transmission increases the basic reproduction number R_0. Furthermore, in Fig. 5.3, we have seen that increasing the quarantine of exposed individuals reduces the amount of basic reproduction number R_0, but only this is not enough to control the COVID-19 outbreak. From our sensitivity analysis, we found that R_0 is most sensitive to the parameters β, τ, q_1, η_2, η_3, and α. This shows us the effectiveness of quarantine of exposed and isolation individuals via healthcare treatment in controlling the pandemic.

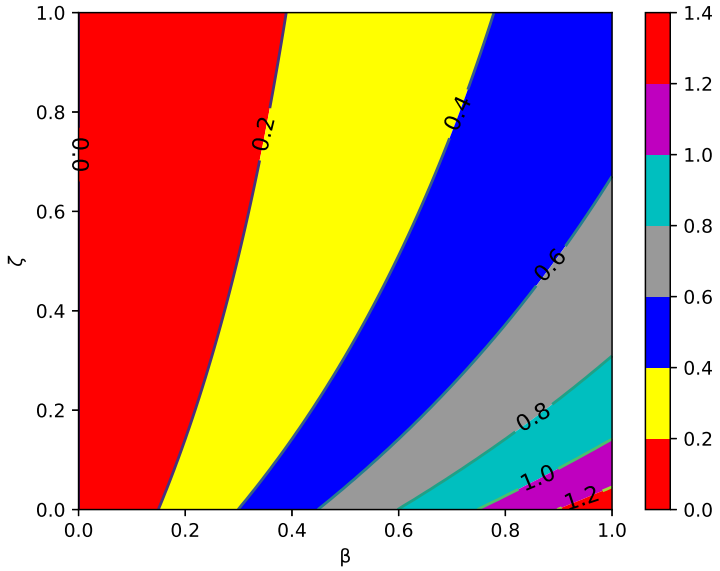

Figure 5.2: Contour plots of R_0 versus transmission rate (β) and quarantine individuals become again susceptible (ζ). All parameter values are given in Table 5.3 except the varied parameters.

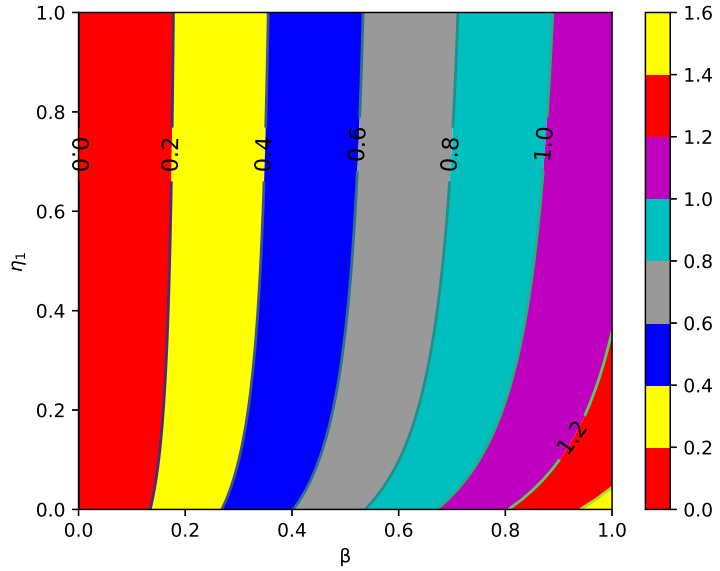

Figure 5.3: Contour plots of R_0 versus transmission rate (β) and exposed individuals become quarantined at rate η_1. All parameter values are given in Table 5.3 except the varied parameters.

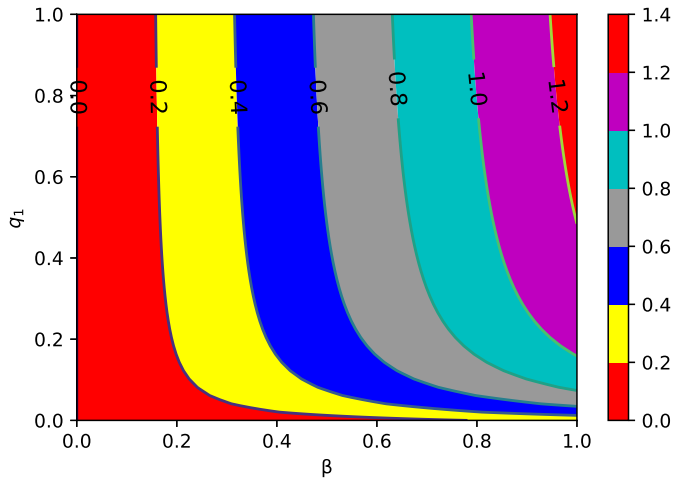

Figure 5.4: Contour plots of R_0 versus transmission rate (β) and quarantined individuals become showing symptoms at rate q_1. All parameter values are given in Table 5.3 except the varied parameters.

The contour in Fig. 5.4 show that when the rate of transfer of individuals becoming infected from quarantined is reduced together with transmission coefficient, then the amount of basic reproduction number R_0 is also reduced. From Fig. 5.5, we can see that increasing the quarantine of exposed individuals and the decrease of quarantined individuals showing symptoms reduces the basic reproduction number and, therefore, COVID-19 cases. From Fig. 5.6, we can see that decreasing the coefficient of transmission and modification factor for asymptomatic coefficient reduces the basic reproduction number and, consequently, the COVID-19 burden would be reduced.

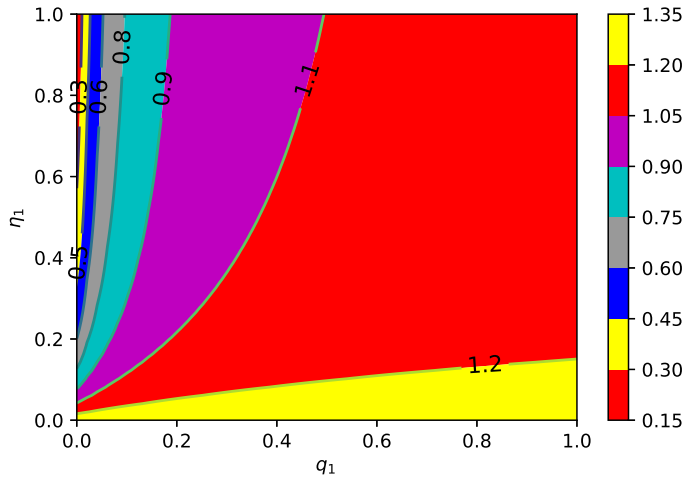

Figure 5.5: Contour plots of R_0 versus quarantined individuals showing symptoms (q_1) and exposed individuals become quarantined at rate η_1. All parameter values are given in Table 5.3 except the varied parameters.

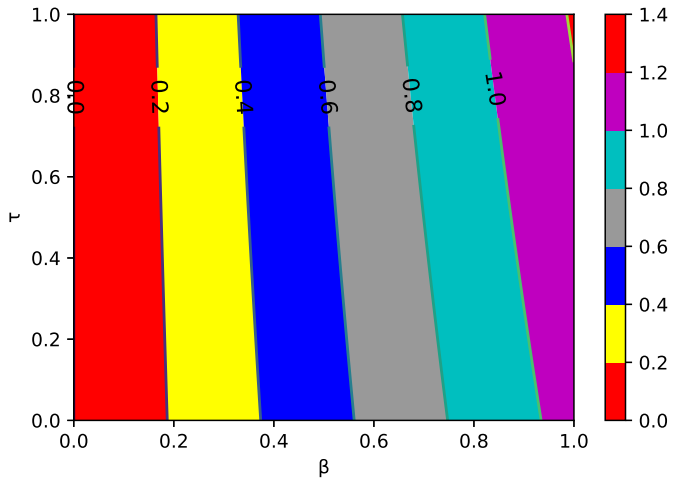

Figure 5.6: Contour plots of R_0 versus transmission rate (β) and modification factor for asymptomatic exposed individuals at rate τ. All parameter values are given in Table 5.3 except the varied parameters.

Further, Fig. 5.7 reveals the variation of R_0 with respect to transmission rate β. It can easily be observed that R_0 increases with an increase in transmission rate β and after a certain value of β, R_0 becomes greater than 1. It implies that up to a certain value of β, disease-free equilibrium is stable and beyond that value of β, disease-free equilibrium becomes unstable.

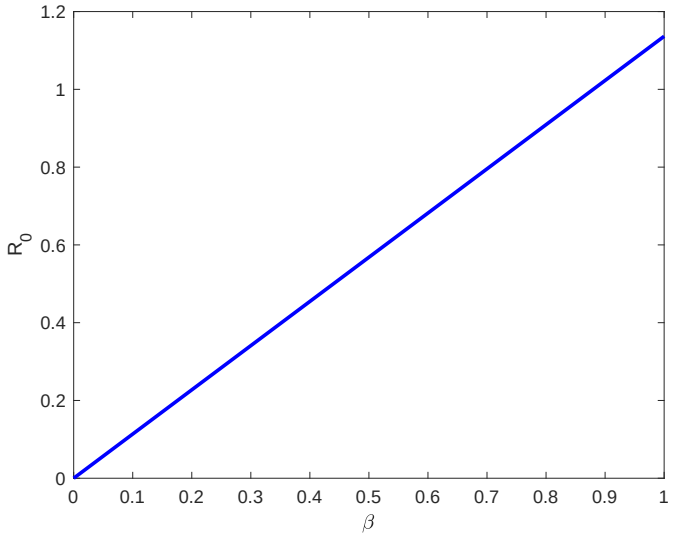

Figure 5.7: Variation of R_0 with respect to coefficient of transmission β.

5.5 Numerical Simulation

In this section, the numerical simulation is performed to support the analytical results. To validate the local stability of DFE of model (5.1), we choose $\beta = 0.65$, and the other parametric

values are similar to the baseline values given in Table 5.3. For E^0, the reproduction number $R_0 = 0.7387$ and DFE, $E^0 = (114963588, 0, 0, 0, 0, 0, 0)$. The local stability of DFE for the model (5.1) is portrayed in Fig. 5.8. In this figure, the infective population gradually tend to disease-free equilibrium.

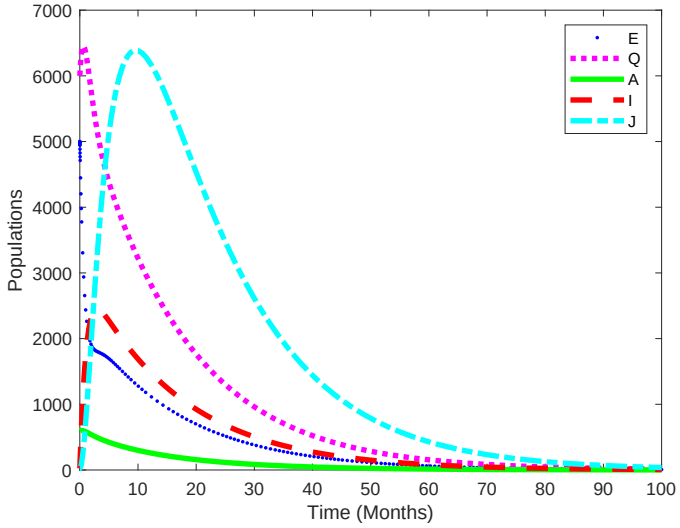

Figure 5.8: The local stability of DFE for the model (5.1). Parameter values used are those given in Table 5.3 except for $\beta = 0.65$, so that $R_0 = 0.7387 < 1$.

For EE we have, $E_1^* = (1.149630984 \times 10^8, 2638, 5604, 382, 2789, 10303, 150773)$ and the reproduction number $R_0 = 1.0029$. The local stability of EE for the model (5.1) is portrayed in Fig. 5.9. In this figure, all the distinct classes coexist in the population and approach endemic equilibrium.

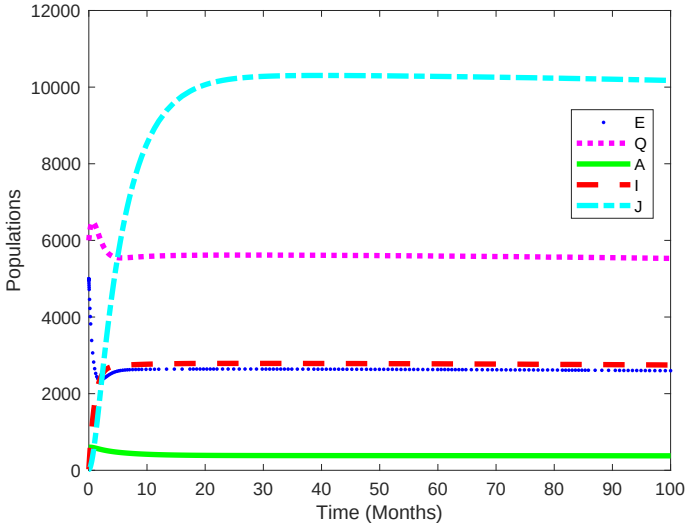

Figure 5.9: The local stability of EE for the model (5.1). Parameter values used are those given in Table 5.3 such that $R_0 = 1.0029 > 1$.

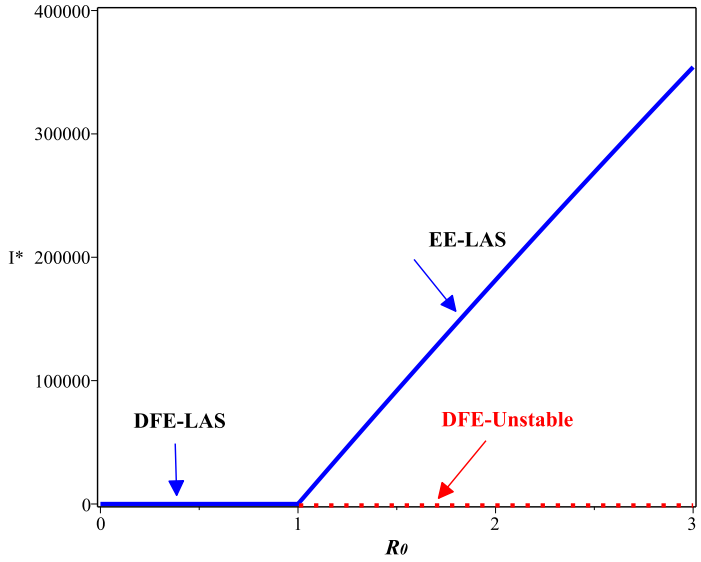

Figure 5.10: Transcritical bifurcation of the model (5.1) when $R_0 = 1$.

The occurrence of the transcritical bifurcation at $R_0 = 1$ for the model (5.1) is illustrated in Fig. 5.10. Precisely, when $R_0 < 1$, the model (5.1) has no endemic equilibrium and the disease-free equilibrium is stable. When $R_0 > 1$, a stable endemic equilibrium appears and the disease-free equilibrium becomes unstable, i.e., the exchange of stability of the equilibrium (transcritical bifurcation) arises.

The global stability (Theorem 8) of the COVID-19-free equilibrium is illustrated in Fig. 5.11. From this figure, we observe that for different initial sizes of the infectious individuals in the population, all solution trajectories converge to the COVID-19-free equilibrium.

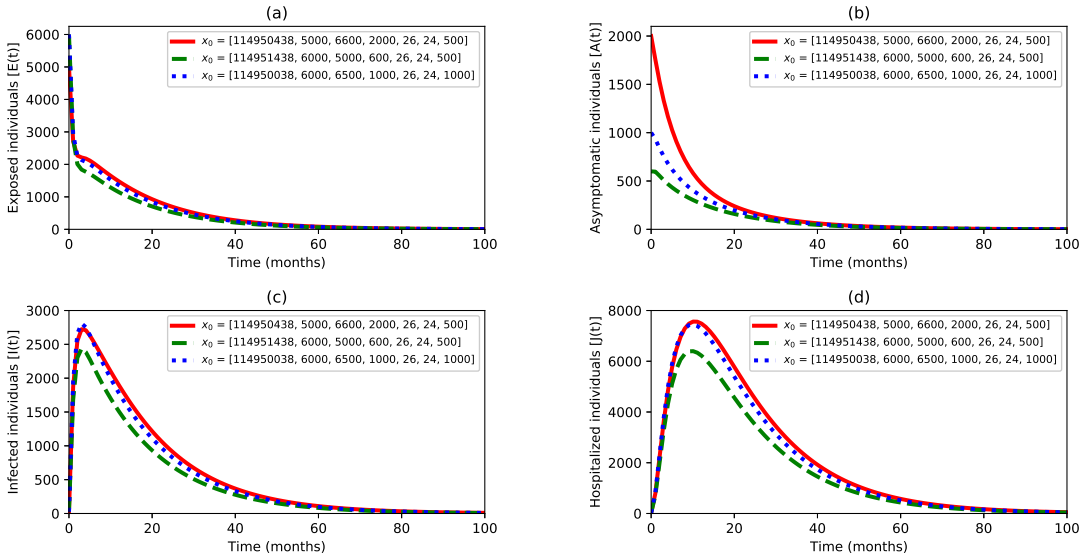

Figure 5.11: Convergence of solution trajectories for **(a)** exposed, **(b)** asymptomatic, **(c)** infected and **(d)** hospitalized individuals at different initial values in line with Theorem 8 by using parameter values given in Table 5.3 except for $\beta = 0.65$, so that $R_0 = 0.7387 < 1$.

In Fig. 5.12, the effects of coefficient of transmission at different values are displayed. It is observed that reducing the coefficient of transmission reduces the burden of infected individuals in hospital. Thus, this graphical suggests that the Ethiopian government takes progressive control measures to reduce the contact rate.

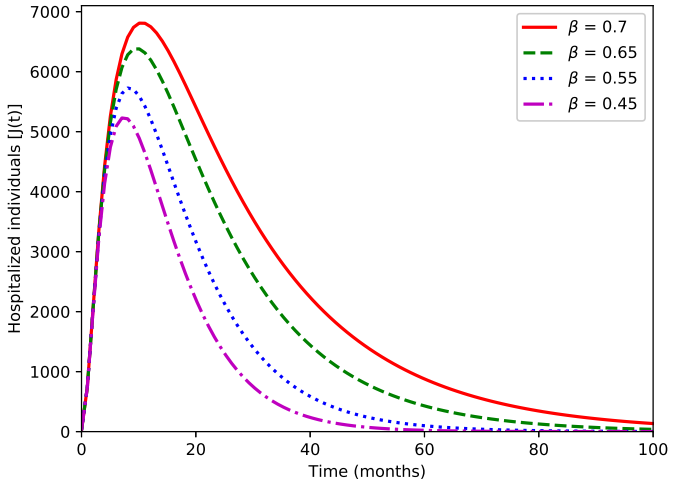

Figure 5.12: Projections with varying effect of coefficient of transmission at values of $\beta = [0.70(R_0 = 0.7955 < 1), 0.65(R_0 = 0.7386 < 1), 0.55(R_0 = 0.6250 < 1), 0.45(R_0 = 0.5114 < 1)]$.

In Fig. 5.13, the effects of the modification factor on asymptomatic coefficient at different values are displayed. The projection shows that the cumulative number of individuals becoming

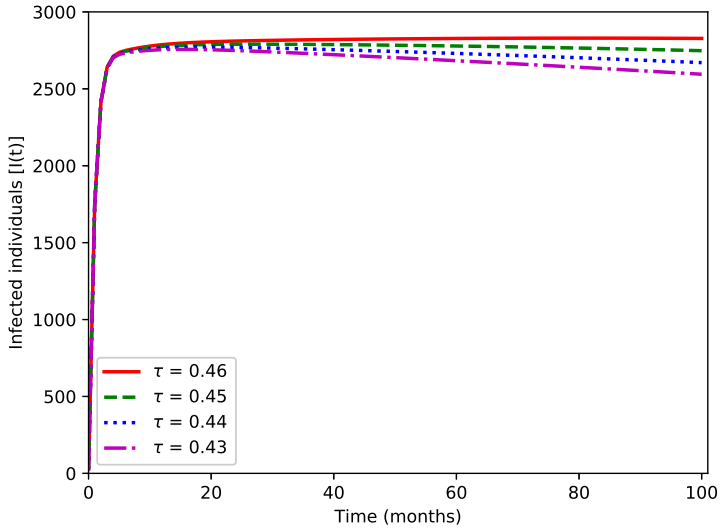

Figure 5.13: Projections with varying effect of modification factor for asymptomatic coefficient at values of $\tau = [0.46(R_0 = 1.0014 > 1), 0.45(R_0 = 1.0029 > 1), 0.44(R_0 = 0.9988 < 1), 0.43(R_0 = 0.9975 < 1)]$.

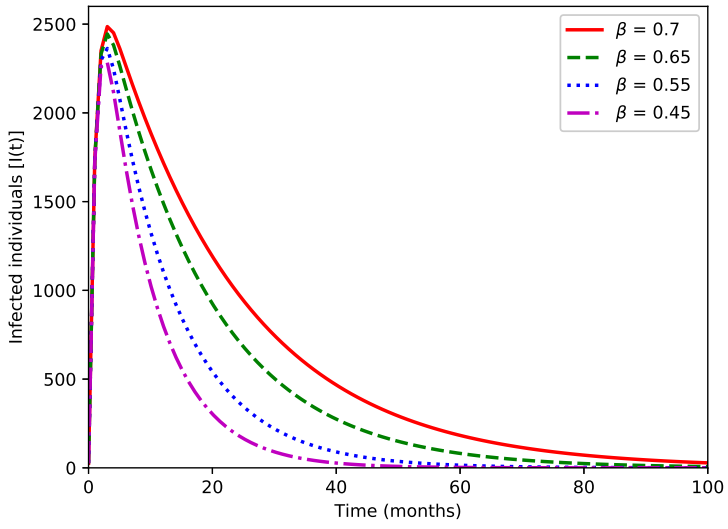

Figure 5.14: Projections with varying effect of coefficient of transmission at values of $\beta = [0.70(R_0 = 0.7955 < 1), 0.65(R_0 = 0.7386 < 1), 0.55(R_0 = 0.6250 < 1), 0.45(R_0 = 0.5114 < 1)]$.

infected is high when τ becomes high and becomes decreasing with low values of τ, which minimize also the values of basic reproduction number less than one. As shown in Fig. 5.14, when the contact rate increases, the number of infected individuals become high and decreasing the value of β decreases the number of infected population. This shows that the infected people with symptoms are significantly contributing the disease burden in the Ethiopian community.

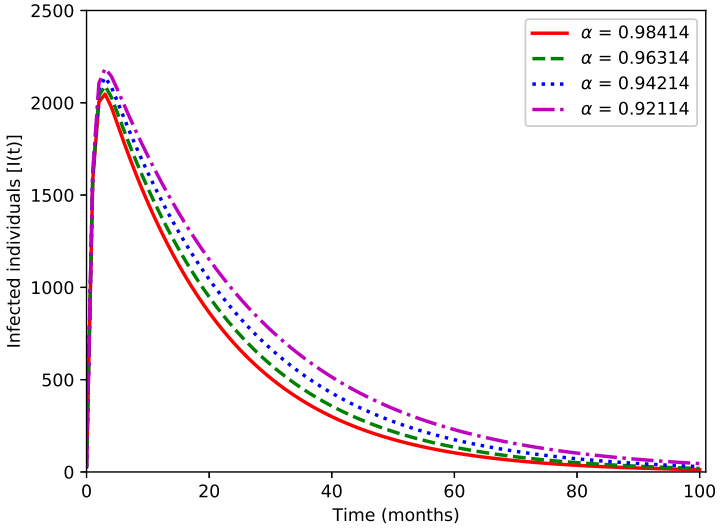

Figure 5.15: Projections with varying effect of infected individuals become exposed to healthcare treatment at values of $\alpha = [0.98414(R_0 = 0.7804 < 1), 0.96314(R_0 = 0.7959 < 1), 0.94214(R_0 = 0.8122 < 1), 0.92114(R_0 = 0.8292 < 1)]$.

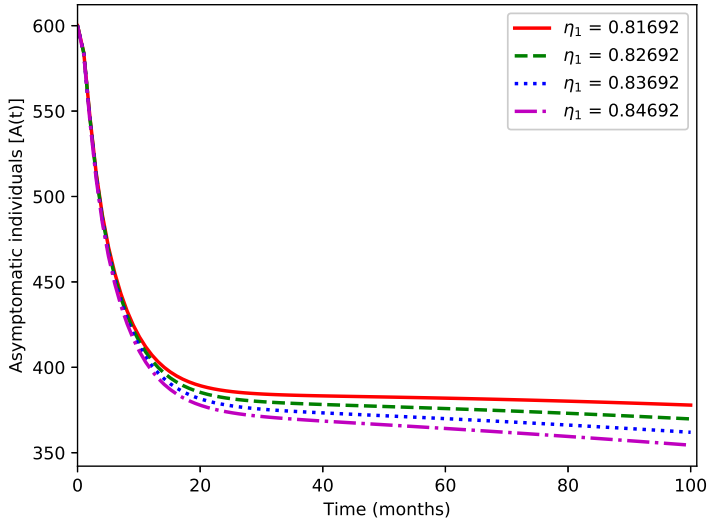

Figure 5.16: Projections with varying effect of quarantine rate of exposed individuals at values of $\eta_1 = [0.81692(R_0 = 1.0029 > 1), 0.82692(R_0 = 0.9994 < 1), 0.83692(R_0 = 0.9987 < 1), 0.84692(R_0 = 0.9981 < 1)]$.

From Fig. 5.15 we observe that increasing the rate of infected individuals exposed to healthcare treatment will decrease the transmission rate from the infected people to susceptible individuals. This implies that isolation of the infected human overall can reduce the risk of future COVID-19 spread in Ethiopia. In Fig. 5.16, we can see that when the rate of exposed individuals becoming quarantined is increased, then the number of individuals getting COVID-19 disease will decrease. Therefore, by increasing the quarantine of exposed individuals, we can minimize the spread of COVID-19 pandemic.

CHAPTER 6

CONCLUSION AND RECOMMENDATION

6.1 Discussion and Conclusions

In the first phase, an optimal control problem is formulated and analyzed in the context of COVID-19 outbreak. Preventive measures(quarantine, isolation, social distancing), surface disinfection to reduce contact rates and intensive medical care are the three candidates for control measures. An expression for the basic reproduction number is derived in terms of control variables. Then the sensitivity of basic reproduction number with respect to model parameters is also analyzed. The optimal control strategies are found by minimizing the number of exposed and infected population taking into account the cost of implementation. The existence of optimal controls and characterization is established with the help of Pontryagin's Maximum Principle. Further, three different simulation cases were comparatively performed to obtain the best control strategies. In general, the numerical simulation results demonstrate good agreement with our analytical results. In addition, the effect of control functions on the basic reproduction number is numerical investigated to determine the prevalence of the disease.

The results of this study also reveals that intensive prevention and medical care are also good control option in the absence of sufficient resource for surface disinfection to minimize the number of exposed and infected population. Finally, from the findings of this study, we came to conclude that the comprehensive impacts of three strategies outperform in reducing the disease epidemic with optimum implementation cost.

In the second phase, we formulated and analyzed a nonlinear deterministic mathematical model to investigate the transmission dynamics of COVID-19. We first obtained the feasible region where the model is epidemiologically and mathematically well-posed. Then, the basic reproduction number, R_0 is computed using the next-generation matrix method. We then analyzed both local and global stability of the the disease-free equilibrium point based on R_0. The analytical result shows that the COVID-19-free equilibrium point is locally as well as globally asymptotically stable if $R_0 < 1$ and unstable if $R_0 > 1$. The existence and stability of the endemic equilibrium point was determined by using the method stated in Castillo-Chavez and Song. Besides, the coexistence equilibrium point is locally asymptotically stable if $R_0 > 1$. From the epidemiological point of view, the disease can be managed if R_0 is less than unity. Otherwise, the disease can persist in the community. We also proved that the model exhibits forward bifurcation with the help of center manifold theory.

In Subsection 5.3, the model parameters are fitted using COVID-19 infected data reported from March 13, 2020 to July 31, 2021 in Ethiopia. In Subsection 5.4, the normalized sensitivity

indices of R_0 show that the most sensitivity parameters are β and τ with positive sign, which shows that decreasing the contact rate with infected and asymptomatic individuals reduces R_0 and so does the disease load. Again, the parameters η_1 and α are the most sensitive parameters with negative sign. This indicates that the increase of quarantine of exposed and treating infected individuals decreases the contact rate which in turn reduces R_0 and so does the disease load.

We performed the numerical simulation in Subsection 5.5. The simulation result shows that the diseases always persist in the community whenever the reproduction number exceeds unity. This supports the fact that decrease in the transmission rate β reduces the value of R_0. Moreover, the decrease in the parameter τ (the modified contact rate at which the asymptomatic individuals interact with susceptible) also shows a positive impact on R_0. In addition, an increase in the parameter η_1 which is the rate that exposed individuals become quarantined, reduces the value of R_0. Thus, the simulation result concludes that the spread of COVID-19 can be managed via minimizing the contact rate of infected and increasing the quarantine of exposed individuals. In the future, it is reasonable extending the present mathematical model via vaccination into an optimal control problem to investigate optimal intervention strategies.

6.2 Recommendation

The simulation result illustrated in Fig.4.5 shown that the number of exposed and infected individuals are highly reduced. Besides, the magnitude of $\mathcal{R}_0$ is lower than unity without utilizing surface disinfection to clean environmental reservoir. Hence, the government needs to exert intensive prevention such as quarantine, isolation, social distancing and medical care simultaneously in the absence sufficient resource for surface disinfection. Furthermore, quantitative results also reveals that the disease persist in the community whenever the reproduction number exceeds unity which depends on the transmission rate β and modified contact rate τ at which the asymptomatic individuals interact with susceptible. In addition, an increase in the parameter η_1 reduces the value of R_0. Hence, this calls for intensive public awareness raising in order to minimizing these contact rates to effectively manage the spread of COVID-19.

REFERENCES

Ahmed, E., & El-Saka, H. (2017). On a fractional order study of middle east respiratory syndrome corona virus (mers-cov). *J. Fract. Calc. Appl*, *8*(1), 118–126.

Ahmed, I., Modu, G. U., Yusuf, A., Kumam, P., & Yusuf, I. (2021). A mathematical model of coronavirus disease (covid-19) containing asymptomatic and symptomatic classes. *Results in physics*, *21*, 103776.

Aldila, D., Ndii, M. Z., & Samiadji, B. M. (2020). Optimal control on COVID-19 eradication program in Indonesia under the effect of community awareness. *Mathematical Biosciences and Engineering*, *17*, 6355–6389.

Ali, M., Shah, S. T. H., Imran, M., & Khan, A. (2020). The role of asymptomatic class, quarantine and isolation in the transmission of COVID-19. *Journal of Biological Dynamics*, *14*(1), 389–408.

Allen, L. J. (2007). *Introduction to Mathematical Biology*. Pearson/Prentice Hall.

Anderson, R. M., Anderson, B., & May, R. M. (1992). *Infectious diseases of humans: dynamics and control*. Oxford university press.

Area, I., Ndairou, F., Nieto, J. J., Silva, C. J., & Torres, D. F. (2017). Ebola model and optimal control with vaccination constraints. *arXiv preprint arXiv:1703.01368*.

Authority, E. F. S., for Disease Prevention, E. C., Control, for Avian Influenza, E. U. R. L., Adlhoch, C., Fusaro, A., ... others (2021). Avian influenza overview december 2020–february 2021. *Efsa Journal*, *19*(3), e06497.

Bajiya, V. P., Bugalia, S., & Tripathi, J. P. (2020). Mathematical modeling of COVID-19: Impact of non-pharmaceutical interventions in India. *Chaos: An Interdisciplinary Journal of Nonlinear Science*, *30*(11), 113143.

Bugalia, S., Bajiya, V. P., Tripathi, J. P., Li, M.-T., & Sun, G.-Q. (2020). Mathematical modeling of COVID-19 transmission: the roles of intervention strategies and lockdown. *Mathematical Biosciences and Engineering*, *17*(5), 5961–5986.

by the Center for Systems Science, J. H. U. C.-. D., & at Johns Hopkins University (JHU, E. C. (2021). *Johns hopkins university corona virus resource center.*

Cai, L., Li, X., Tuncer, N., Martcheva, M., & Lashari, A. A. (2017). Optimal control of a malaria model with asymptomatic class and superinfection. *Mathematical biosciences*, *288*, 94–108.

Castillo-Chavez, C., & Song, B. (2004). Dynamical models of tuberculosis and their applications. *Mathematical Biosciences & Engineering*, *1*(2), 361.

Catrin Sohrabi, N. O. M. K. A. K.-A. A.-J. C. I., Zaid Alsafi, & Agha., R. (2020). World health organization declares global emergency: A review of the 2019 novel coronavirus (covid-19). *International Journal of Surgery*.

CDC. (2019). Centers for Disease Control and Prevention (CDC), Symptoms of Coronavirus, available from: https://bit.ly/3KegjEA.

Chen, T.-M., Rui, J., Wang, Q.-P., Zhao, Z.-Y., Cui, J.-A., & Yin, L. (2020). A mathematical model for simulating the phase-based transmissibility of a novel coronavirus. *Infectious diseases of poverty*, *9*(1), 1–8.

Chitnis, N., Hyman, J. M., & Cushing, J. M. (2008). Determining important parameters in the spread of malaria through the sensitivity analysis of a mathematical model. *Bulletin of Mathematical Biology*, *70*(5), 1272.

Coddington, E. A., & Levinson, N. (1955). *Theory of Ordinary Differential Equations*. Tata McGraw-Hill Education.

Cucinotta, D., & Vanelli, M. (2020). Who declares covid-19 a pandemic. *Acta Bio Medica: Atenei Parmensis*, *91*(1), 157.

Das, D. K., Khajanchi, S., & Kar, T. K. (2020). The impact of the media awareness and optimal strategy on the prevalence of tuberculosis. *Applied Mathematics and Computation*, *366*, 124732.

Debela, B. K. (2020). The covid-19 pandemic and the ethiopian public administration: responses and challenges. *Good Public Governance in a Global Pandemic*, *113*.

Deressa, C. T., & Duressa, G. F. (2021). Modeling and optimal control analysis of transmission dynamics of COVID-19: The case of Ethiopia. *Alexandria Engineering Journal*, *60*(1), 719–732.

Diekmann, O., Heesterbeek, J., & Roberts, M. G. (2010). The construction of next-generation matrices for compartmental epidemic models. *Journal of the Royal Society Interface*, *7*(47), 873–885.

Eikenberry, S. E., Mancuso, M., Iboi, E., Phan, T., Eikenberry, K., Kuang, Y., ... Gumel, A. B. (2020). To mask or not to mask: Modeling the potential for face mask use by the general public to curtail the COVID-19 pandemic. *Infectious Disease Modelling*, *5*, 293–308.

Ethiopia, U. (2020). Socio-economic impacts of covid-19 update-14th may 2020. *Update*.

Fleming, W. H., & Rishel, R. W. (2012). *Deterministic and stochastic optimal control* (Vol. 1). Springer Science & Business Media.

Ge, F., Zhang, D., Wu, L., & Mu, H. (2020). Predicting psychological state among chinese undergraduate students in the covid-19 epidemic: a longitudinal study using a machine learning. *Neuropsychiatric disease and treatment*, *16*, 2111.

Gralinski, L. E., & Menachery, V. D. (2020). Return of the coronavirus: 2019-ncov. *Viruses*, *12*(2), 135.

Guckenheimer, J., & Holmes, P. (2013). *Nonlinear oscillations, dynamical systems, and bifurcations of vector fields* (Vol. 42). Springer Science & Business Media.

Hale, J. (1969). *Ordinary Differential Equations, in: Pure and Applied Mathematics.* Wiley-Interscience, New York.

Hanscheid, T., Valadas, E., & Grobusch, M. P. (2020). Coronavirus 2019-ncov: Is the genie already out of the bottle? *Travel medicine and infectious disease*, *35*, 101577.

Hethcote, H. W. (2000). The mathematics of infectious diseases. *SIAM review*, *42*(4), 599–653.

Hui, D. S., Azhar, E. I., Madani, T. A., Ntoumi, F., Kock, R., Dar, O., ... others (2020). The continuing 2019-ncov epidemic threat of novel coronaviruses to global health—the latest 2019 novel coronavirus outbreak in wuhan, china. *International journal of infectious diseases*, *91*, 264–266.

Kampf, G., Todt, D., Pfaender, S., & Steinmann, E. (2020). Persistence of coronaviruses on inanimate surfaces and their inactivation with biocidal agents. *Journal of hospital infection*, *104*(3), 246–251.

Kermack, W. O., & McKendrick, A. G. (1927). A contribution to the mathematical theory of epidemics. *Proceedings of the royal society of london. Series A, Containing papers of a mathematical and physical character*, *115*(772), 700–721.

Khan, M., Shah, S. W., Ullah, S., & Gómez-Aguilar, J. (2019). A dynamical model of asymptomatic carrier zika virus with optimal control strategies. *Nonlinear Analysis: Real World Applications*, *50*, 144–170.

Kim, S., Aurelio, A., & Jung, E. (2018). Mathematical model and intervention strategies for mitigating tuberculosis in the philippines. *Journal of theoretical biology*, *443*, 100–112.

Kim, Y., Lee, S., Chu, C., Choe, S., Hong, S., & Shin, Y. (2016). The characteristics of middle eastern respiratory syndrome coronavirus transmission dynamics in south korea. *Osong public health and research perspectives*, *7*(1), 49–55.

Kucharski, A. J., Russell, T. W., Diamond, C., Liu, Y., Edmunds, J., Funk, S., ... others (2020). Early dynamics of transmission and control of covid-19: a mathematical modelling study. *The lancet infectious diseases*, *20*(5), 553–558.

Kumar, A., Srivastava, P. K., Dong, Y., & Takeuchi, Y. (2020). Optimal control of infectious disease: Information-induced vaccination and limited treatment. *Physica A: statistical mechanics and its applications*, *542*, 123196.

Lee, D., Masud, M., Kim, B. N., & Oh, C. (2017). Optimal control analysis for the mers-cov outbreak: South korea perspectives. *Journal of the Korean Society for Industrial and Applied Mathematics*, *21*(3), 143–154.

Legesse, L. O., & Shiferaw, F. B. (2020). Optimal control strategies for the transmission risk of COVID-19. *Journal of Biological Dynamics*, *14*(1), 590–607.

Lemos-Paião, A. P., Silva, C. J., & Torres, D. F. (2017). An epidemic model for cholera with optimal control treatment. *Journal of Computational and Applied Mathematics*, *318*, 168–180.

Lenhart, S., & Workman, J. T. (2007). *Optimal Control Applied to Biological Models*. Chapman and Hall/CRC.

Li, Q., Guan, X., Wu, P., Wang, X., Zhou, L., Tong, Y., ... others (2020). Early transmission dynamics in wuhan, china, of novel coronavirus–infected pneumonia. *New England Journal of Medicine*, *368*(6490), 489–493.

Li, R., Pei, S., Chen, B., Song, Y., Zhang, T., Yang, W., & Shaman, J. (n.d.). Substantial undocumented infection facilitates the rapid dissemination of novel coronavirus (sars-cov-2). *Science*.

Li, Y., & Muldowney, J. S. (1993). On bendixson s criterion. *Journal of Differential Equations*, *106*(1), 27–39.

Lin, Q., Zhao, S., Gao, D., Lou, Y., Yang, S., Musa, S. S., ... others (2020). A conceptual model for the coronavirus disease 2019 (covid-19) outbreak in wuhan, china with individual reaction and governmental action. *International journal of infectious diseases*, *93*, 211–216.

Makinde, O. D., & Okosun, K. O. (2011). Impact of chemo-therapy on optimal control of malaria disease with infected immigrants. *BioSystems*, *104*(1), 32–41.

Massinga Loembé, M., Tshangela, A., Salyer, S. J., Varma, J. K., Ouma, A. E. O., & Nkengasong, J. N. (2020). Covid-19 in africa: the spread and response. *Nature Medicine*, *26*(7), 999–1003.

Memon, Z., Qureshi, S., & Memon, B. R. (2021). Assessing the role of quarantine and isolation as control strategies for COVID-19 outbreak: a case study. *Chaos, Solitons & Fractals*, *144*, 110655.

Mizumoto, K., & Chowell, G. (2020). Transmission potential of the novel coronavirus (covid-19) onboard the diamond princess cruises ship, 2020. *Infectious Disease Modelling*, *5*, 264–270.

Mohammed-Awel, J., & Gumel, A. B. (2019). Mathematics of an epidemiology-genetics model for assessing the role of insecticides resistance on malaria transmission dynamics. *Mathematical biosciences*, *312*, 33–49.

Musa, S. S., Qureshi, S., Zhao, S., Yusuf, A., Mustapha, U. T., & He, D. (2021). Mathematical modeling of COVID-19 epidemic with effect of awareness programs. *Infectious Disease Modelling*, *6*, 448–460.

Mussie, K. M., Gradmann, C., & Manyazewal, T. (2020). Bridging the gap between policy and practice: a qualitative analysis of providers' field experiences tinkering with directly observed therapy in patients with drug-resistant tuberculosis in addis ababa, ethiopia. *BMJ open*, *10*(6), e035272.

Nadim, S. S., & Chattopadhyay, J. (2020). Occurrence of backward bifurcation and prediction of disease transmission with imperfect lockdown: A case study on COVID-19. *Chaos, Solitons & Fractals*, *140*, 110163.

Ngonghala, C. N., Iboi, E., Eikenberry, S., Scotch, M., MacIntyre, C. R., Bonds, M. H., & Gumel, A. B. (2020). Mathematical assessment of the impact of non-pharmaceutical interventions on curtailing the 2019 novel coronavirus. *Mathematical biosciences*, *325*, 108364.

Olaniyi, S., Obabiyi, O., Okosun, K., Oladipo, A., & Adewale, S. (2020). Mathematical modelling and optimal cost-effective control of covid-19 transmission dynamics. *The European Physical Journal Plus*, *135*(11), 1–20.

Organization, W. H. (2020). *Coronavirus disease 2019 (covid-19): situation report, 105* (Tech. Rep.). WHO.

Pan, X., Ojcius, D. M., Gao, T., Li, Z., Pan, C., & Pan, C. (2020). Lessons learned from the 2019-ncov epidemic on prevention of future infectious diseases. *Microbes and infection*, *22*(2), 86–91.

Pontryagin, L. S., Boltyanskii, V., Gamkrelidze, R., Mishchenko, E., Trirogoff, K., & Neustadt, L. (2018). *Ls pontryagin selected works: The mathematical theory of optimal processes*. Routledge.

Rothe, C., Schunk, M., Sothmann, P., Bretzel, G., Froeschl, G., Wallrauch, C., ... others (2020). Transmission of 2019-nCoV infection from an asymptomatic contact in Germany. *New England Journal of Medicine*, *382*(10), 970–971.

Silva, C. J., & Torres, D. F. (2013). Optimal control for a tuberculosis model with reinfection and post-exposure interventions. *Mathematical Biosciences*, *244*(2), 154–164.

Tahir, M., Shah, S. I. A., Zaman, G., & Khan, T. (2019). Stability behaviour of mathematical model mers corona virus spread in population. *Filomat*, *33*(12), 3947–3960.

Tang, B., Bragazzi, N. L., Li, Q., Tang, S., Xiao, Y., & Wu, J. (2020). An updated estimation of the risk of transmission of the novel coronavirus (2019-nCov). *Infectious Disease Modelling*, *5*, 248–255.

Tang, B., Wang, X., Li, Q., Bragazzi, N. L., Tang, S., Xiao, Y., & Wu, J. (2020). Estimation of the transmission risk of the 2019-nCoV and its implication for public health interventions. *Journal of clinical medicine*, *9*(2), 462.

Tilahun, G. T., & Alemneh, H. T. (2021). Mathematical modeling and optimal control analysis of covid-19 in ethiopia. *Journal of Interdisciplinary Mathematics*, *24*(8), 2101–2120.

Ullah, S., & Khan, M. A. (2020). Modeling the impact of non-pharmaceutical interventions on the dynamics of novel coronavirus with optimal control analysis with a case study. *Chaos, Solitons & Fractals*, *139*, 110075.

Van den Driessche, P., & Watmough, J. (2002). Reproduction numbers and sub-threshold endemic equilibria for compartmental models of disease transmission. *Mathematical Biosciences*, *180*(1-2), 29–48.

Worldometer. (2020). Worldometer, coronavirus incubation period, available from: https://www.worldometers.info/coronavirus/coronavirus-incubation-period/.

Wu, J. T., Leung, K., & Leung, G. M. (2020). Nowcasting and forecasting the potential domestic and international spread of the 2019-nCoV outbreak originating in Wuhan, China: a modelling study. *The Lancet*, *395*(10225), 689–697.

Yang, C., & Wang, J. (2020). A mathematical model for the novel coronavirus epidemic in Wuhan, China. *Mathematical Biosciences and Engineering: MBE*, *17*(3), 2708.

Yazew, B. G., Abate, H. K., & Mekonnen, C. K. (2021). Knowledge, attitude and practice towards covid-19 in ethiopia: a systematic review; 2020. *Patient preference and adherence*, *15*, 337.